










Breeder blanket and tritium fuel cycle feasibility of the Infinity Two fusion pilot plant

D.W.S. Clark¹ , B. Goh¹ , S. Ramirez¹, E. Pflug², J. Smandych², J.R. Kessing¹ , C. Moreno², T.D. Bohm², P.P.H. Wilson² , L. Singh¹ , A. Cerfon¹ , N.R. Mandell¹ , J.C. Schmitt¹ , W. Gutfenfelder¹ , C. Lau¹, M.S. Tillack¹ and J.M. Canik¹

¹Type One Energy Group Inc., Knoxville, TN, USA

²Department of Nuclear Engineering & Engineering Physics, University of Wisconsin, Madison, WI, USA

Corresponding author: D.W.S. Clark, daniel.clark@typeoneenergy.com

(Received 3 December 2024; revision received 17 March 2025; accepted 18 March 2025)

The selection, design and optimization of a suitable blanket configuration for an advanced high-field stellarator concept is seen as a key feasibility issue and has been incorporated as a vital and necessary part of the Infinity Two fusion pilot plant physics basis. The focus of this work was to identify a baseline blanket which can be rapidly deployed for Infinity Two while also maintaining flexibility and opportunities for higher performing concepts later in development. Results from this analysis indicate that gas-cooled solid breeder designs such as the helium-cooled pebble bed (HCPB) are the most promising concepts, primarily motivated by the neutronics performance at applicable blanket build depths, and the relatively mature technology basis. The lithium lead (PbLi) family of concepts, particularly the dual-cooled lithium lead, offer a compelling alternative to solid blanket concepts as they have synergistic developmental pathways while simultaneously mitigating much of the technical risk of those designs. Homogenized three-dimensional neutronics analysis of the Infinity Two configuration indicates that the HCPB achieves an adequate tritium breeding ratio (TBR) (1.30 which enables sufficient margin at low engineering fidelity), and near appropriate shielding of the magnets (average fast fluence of $1.3 \times 10^{18} \text{ n cm}^{-2}$ per full-power year). The thermal analysis indicates that reasonably high thermal efficiencies (greater than 30 %) are readily achievable with the HCPB paired with a simple Rankine cycle using reheat. Finally, the tritium fuel cycle analysis for Infinity Two shows viability, with anticipated operational inventories of less than one kilogram (approximately 675 g) and a required TBR (TBR_{req}) of less than 1.05 to maintain fuel self-sufficiency (approximately 1.023 for a driver blanket with no inventory doubling). Although further optimization and engineering design are still required, at the physics basis stage all initial targets have been met for the Infinity Two configuration.

Keywords: fusion plasma

1. Introduction

The stellarator has many unique features that makes it attractive as a fusion energy system. Stellarators are intrinsically steady state, can operate at high plasma density to achieve high gain while potentially relaxing plasma exhaust constraints, have relatively benign responses to magnetohydrodynamic (MHD) instabilities, avoid current-driven disruptions and have low recirculating power requirements. These benefits all provide an opportunity to develop a net electric pilot plant at reduced risk and low capital cost (Gates *et al.* 2018; Baalrud *et al.* 2020). The key tradeoff for these benefits is a highly non-uniform three-dimensional plasma shape and coil configuration, which adds challenges with regards to modeling, design integration, fabrication and maintenance of integrated stellarator systems (Gates *et al.* 2018). In the near term, this requires the development of new tools and approaches to be able to adequately assess and modify blanket designs for stellarators (Häußler *et al.* 2018; Palermo *et al.* 2021; Lyytinen *et al.* 2024; Palermo *et al.* 2024). Regardless of confinement concept, all deuterium-tritium (DT) fusion-based fusion pilot plants (FPPs) require meaningful technological development beyond the burning plasma itself. Critical enabling technologies such as plasma facing components, structural and functional materials and breeding blanket and tritium handling systems need to be further advanced in order to realize reduced-risk commercial systems (US Department of Energy 2021). The breeding blanket and tritium fuel cycle (TFC) related aspects of DT fusion systems in particular embody some of the most fundamental and challenging feasibility and attractiveness issues in the development of commercial fusion energy. Three primary, system driving functions must be satisfied by these components and have strong implications on overall design performance.

The first and most important function relates to the breeding of tritium, which is not naturally occurring in significant quantities and is impossible to stockpile long term due to its short half-life of 12.32 years. The current world-wide tritium inventory is projected to be 30 kg to 40 kg over the next decade, and tritium production in existing CANada Deuterium Uranium (CANDU) fission reactors is less than 0.13 kg per year per reactor (Ni *et al.* 2013; Kovari *et al.* 2018). In contrast, tritium consumption in high availability fusion power systems will be larger than current production, of the order of 5.6 kg per 100 MW_{th} fusion plasma power per full-power year. This drives the requirement that tritium must be bred, extracted and carefully controlled during operation to ensure fuel self-sufficiency and ultimately closure of the DT fuel cycle. Further complicating the matter is the relatively low utilization of tritium in a magnetic fusion energy (MFE) plasma core (order of a fraction to a few percent) which leads to the requirement for effectively and efficiently processing significant amounts of tritium in a continuous fashion (Whyte *et al.* 2023). The amount and throughput of tritium that will need to be managed in a fusion power plant will likely be several orders of magnitude larger than the quantities of tritium that have been handled in existing or planned fusion experiments to date, and although relevant technologies exist, they will need to be scaled up in order to handle the expected throughput of commercial systems. These operational inventories drive key engineering considerations such as the tritium start-up inventory, tritium breeding ratio (TBR), safety and waste, and must be minimized to the extent possible.

In addition to fuel self-sufficiency, the breeder blanket will also play a pivotal role in the overall thermal efficiency of DT fusion energy systems. It must extract

heat originating both from volumetric heat generation caused by neutrons, subsequent prompt photon energy deposition and nuclear reactions inside the blanket as well as plasma radiation towards the first wall, which is typically integrated on the surface of the blanket for neutron economy reasons (Hesch *et al.* 2018). Since the blanket is anticipated to account for 80 %–90 % of the plasma facing surface, the majority of the energy of the DT fusion reaction is imparted into high energy neutrons (approximately 80 %), and MFE systems typically run with a strong radiative fraction (90 %–95 %), it is conservatively estimated that at least 75 % of the overall system heat loads will reside in the blanket. This heat must be effectively removed both for effective thermal conversion but also to keep materials and components within operating temperature limits. This is done through the forced flow of one or more coolants, depending on design. The characteristics of this coolant flow, including pumping power requirements, and its coupling to a thermal conversion system will dictate both power production and overall power conversion efficiency of an energy producing system.

Finally, the breeder blanket will be responsible for providing a significant amount of nuclear shielding for device lifetime components. For MFE devices this typically includes the plasma confining magnetic field coils, which are relatively sensitive to radiation, but can also include other large components such as the vacuum vessel, which may be too costly or difficult to easily replace over the life of the device. A key consideration of any fusion blanket design is its efficacy in both slowing and absorbing neutrons (El-Guebaly 2018; Pereslavytsev *et al.* 2019), given the relatively large penetration length scales of the energetic DT fusion neutrons (order of meters) as well as the requirement to reduce the neutron flux by approximately four orders of magnitude from the first wall to the coil structures. In addition to the minimum blanket volume required for breeding, the optimized shielding performance of the blanket, including any integrated dedicated shield material, will play a factor in determining the minimum allowable plasma-to-magnet spacing and ultimately drive the size of MFE devices such as stellarators. This shielding will also play a vital role in safety and activated material management considerations of a DT energy system.

In addition to serving these core functions, in-vessel components such as the blanket will be subjected to, and must survive, immensely harsh conditions, including a combination of extreme radiation, high heat, mechanical stress and volatile chemical environments. This represents one of the ultimate challenges in materials science and engineering, and it is expected that the performance of these components will ultimately dictate the economic, safety and environmental attractiveness of any given fusion system (Aubert *et al.* 2018). At present, the behavior and reliability of materials subjected to this environment have relatively high uncertainty, and this uncertainty affects design choices as well as research and development (R&D) needs.

For these reasons, the selection, design and optimization of a suitable blanket configuration for an advanced high-field stellarator concept is seen as a key feasibility issue and has been incorporated as a vital and necessary part of the Infinity Two physics basis from the onset. The purpose of this paper is to document at a high level the selection process, including identification of objectives, analyses and findings. As outlined in the overview (Hegna *et al.* 2025), Type One Energy Group Inc. (T1E) is pursuing an ambitious and uniquely direct path to fusion known as the *FusionDirect* program, the cornerstone of which is the disciplined adherence to a technology development path with the lowest possible risk and shortest possible schedule to realize a high-field stellarator FPP. The overarching objective of the

<i>FusionDirect</i> objectives	Blanket and TFC guiding principles
1. Demonstrate safe, stable, steady-state operation taking advantage of a high-field stellarator configuration.	1a. Availability, safety and waste generation should be driving considerations for design choices. 1b. The blanket and other in-vessel components should only use low activation materials. 1c. The blanket and fuel cycle tritium inventories should be minimized as low as is reasonably possible.
2. Demonstrate commercially relevant generation of electricity from DT fusion.	2a. The blanket should enable reasonably high fusion-to-electric power conversion for net electricity generation. 2b. The blanket and associated tritium plant should demonstrate viability of a closed DT fuel cycle. 2c. Design choices should be consistent with a reasonably low overnight capital cost and leveled cost of electricity.
3. Follow the shortest path for development of an FPP to enable deployment by the mid-2030s.	3a. The blanket should not require the development of new structural materials to meet deployment timeline. 3b. External developments should be leveraged where possible. 3c. Developmental pathways should balance developmental vs. performance risk for both Infinity Two and longer-term commercial systems.

TABLE 1. *FusionDirect* objectives and subsequent blanket and TFC guiding principles.

FusionDirect program’s mission is to demonstrate safe, stable, steady-state operation of a high-field stellarator capable of reliably generating clean, sustainable electricity for commercial applications by the mid-2030s. Cascading from this objective, several high-level guidelines were imposed on the T1E blanket and TFC program at an early stage to ensure the technology choices and subsequent technology development program remain compatible with the overarching missions embodied by *FusionDirect*. These guidelines are summarized in [table 1](#).

2. Technical background

Over the past decades countless studies have examined various breeder blanket concepts for both MFE and inertial fusion energy applications. Until a few years ago, the primary drivers of this research were public research organizations involved in government sponsored research world-wide. One of the main focal points of this research is on the development of breeder blanket mock-ups to be tested on the ITER tokamak currently under construction in Cadarache, France, known as the test blanket modules (Giancarli *et al.* 2020). The basic concept of all breeder blankets envisaged for DT fusion focuses on achieving tritium self-sufficiency via conversion of lithium to tritium by means of nuclear reactions. Lithium may be present as a liquid metal, liquid eutectic alloy, molten salt or in solid form such as a lithium-bearing ceramic. At the most fundamental level, a blanket consists of this breeding medium in an assembly fabricated of fusion relevant structural materials, a flowing coolant

Breeder Medium	Lithium	PbLi	FLiBe	Solid
Structural material				
Gen-1 RAFM steels ¹	X	X		X
Advanced steels ²	X	X	X	X
Vanadium alloys	X		X	
SiC/SiC components		X	X	X
Inconel 718 ³			X	
Coolant				
Self	X	X	X	
He	X	X	X	X
Water		X		X
Multiplier				
Be/Beryllides	X		X	X
Self		X	X	
Pb				X
Example concepts	SCLV, SCLFS, He-Li- FS DC, He-Li-V DC	WCLL ⁴ , HCLL, DCLL, LLCB ⁴ , SCYLLA, GAMBL	F-LIB, EBB, LFSC, LFDC	HCPB ⁴ , WCCB ⁴ , HCCR ⁴ , HCCB ⁴ , MLCB ⁴

¹F82H, EUROFER97.

²CNA, ODS.

³Inconel is not considered to be a low activation material.

⁴Blanket concepts currently proposed for the ITER Test Blanket Modules program.

TABLE 2. Primary blanket combinations under consideration in literature.

used to extract heat and a neutron multiplier for increased neutron economy as needed. Families of existing low activation structural materials under consideration include reduced activation ferritic martensitic (RAFM) steels, advanced steels (castable nanostructured alloys (CNAs) and oxide dispersion strengthened (ODS) steels), vanadium alloys or silicon carbide (SiC) based ceramic matrix composites. Coolants under consideration include water, helium (He), carbon dioxide (CO₂) or self-cooling through the flow of liquid breeding media. Neutron multipliers include beryllium and lead-based materials. A non-exhaustive, general summary of popular combinations considered in the literature can be seen in [table 2](#).

In order to help narrow down the field of extremely diverse concepts, six reference concepts were identified from design studies in the literature. These reference concepts are meant to be indicative of the broad ‘family’ of designs defined by the selection of primary components, namely, breeding medium, structure, coolant and neutron multiplier, as well as the relevant regimes in which they are employed. A brief description of each reference concept is included below, and readers are directed to the referenced publications for further details. The first three reference concepts represent some of the most commonly explored designs to date,

mainly owing to their inclusion in both the ITER test blanket modules and international fusion energy programs. The focus of these designs tends to be on near-term technical feasibility.

The helium-cooled pebble bed (HCPB) concept is one of two blanket concepts selected for the EU Demonstration Power Plant (EU DEMO) (Hernández *et al.* 2023). The current reference HCPB design is the so-called ‘pin’ design, which is based on a radial arrangement of ceramic fuel-breeder pins using RAFM structure (EUROFER97) for optimized neutronics performance. Each pin consists of two concentric tubes that form the inner and outer cladding which are filled with the tritium breeding material (Karlsruhe lithium orthosilicate advanced ceramic breeder pebbles). The volume between pins is filled by hexagonal prismatic blocks of neutron multiplier material (Be_{12}Ti). Each pin is cooled with high pressure He. A separate stream of He purge gas doped with hydrogen is flowed through the breeder pins and multiplier prismatic blocks for tritium removal (Hernández *et al.* 2019, 2020; Zhou *et al.* 2023a).

The helium-cooled lithium lead (HCLL) concept was one of the four candidate blankets selected for the EU DEMO prior to down-selection at the preconceptual design phase (Aubert *et al.* 2018). The general concept of the HCLL breeding blanket consists of several boxes stiffened by actively He-cooled plates, between which the PbLi neutron multiplier, tritium breeder and carrier medium slowly flow. The structural material of choice is RAFM steel (EUROFER97). The current reference design is known as the ‘advanced-plus’ HCLL, which is aimed at providing optimized breeding, shielding and thermo-mechanical performance through the implementation of only thin horizontal stiffening plates (Aubert *et al.* 2018; Boullon *et al.* 2019; Jaboulay *et al.* 2019).

The dual coolant lithium lead (DCLL) concept has been considered by a number of public programs including both the EU (Rapisarda *et al.* 2021) and US (Kessel *et al.* 2018) due both to its readiness for deployment as well as to its high degree of design flexibility and potential for extrapolated performance. This blanket concept uses RAFM steels (F82H or EUROFER97) or higher temperature and/or radiation resistant variants (such as the CNA or ODS steels) as structural material. The primary coolant is He and the PbLi liquid metal acts as a breeder, multiplier, tritium carrier medium and secondary coolant. SiC-composite flow channel inserts are typically employed as electrical and thermal insulators between the PbLi and the RAFM steel in the blanket to minimize MHD pressure drops for the liquid metal. The details of the individual DCLL designs can vary widely depending on materials selection, PbLi flow speed and operating temperature (Smolentsev *et al.* 2015). The reference DCLL design used in this analysis was the same as that employed on the US Fusion Nuclear Science Facility (FNSF) study (Kessel *et al.* 2018), which was chosen due to the availability of design details, although higher performing concepts are also under development (Rapisarda *et al.* 2021).

In addition to these more traditional designs, a number of higher-risk, higher-reward concepts have also appeared in the literature. These predominantly focus on self-cooled blankets, which were first conceived in the 1980s as an optimal solution which allows for design simplification and increased performance compared with the separately cooled concepts highlighted in the previous section. The initial design space for these concepts was mostly explored through the US blanket (Smith *et al.* 1985; Raffray *et al.* 2002) and Advanced Research Innovation and Evaluation Study (ARIES) programs (University of Wisconsin-Madison 2024a) due to their potential attractiveness for commercial systems. Currently, no self-cooled blanket

has been developed beyond the concept exploration phase primarily due to the limited need to develop advanced blanket technology for fusion experiments such as ITER (Giancarli *et al.* 2020), but also due to the perceived maturity of suitable materials required for implementing such blanket designs (Raffray *et al.* 2002). The emergence of the fusion private industry has renewed interest in these concepts, with three MFE-relevant designs identified in this study.

The first is the self-cooled lithium lead (SCLL) concept which is being championed by Kyoto Fusioneering (Pearson *et al.* 2022). This design builds on the ARIES-Advanced and Conservative Tokamak (ACT1) blanket concept, which is embodied by the choice of SiC composite structural material and PbLi eutectic, which serves as the breeder, coolant, multiplier and tritium carrier (Kessel *et al.* 2015). An optional additional Be neutron multiplier known as a ‘booster’ or reflector are also variations on the design, which can be included or adjusted based on performance requirements.

The second is the self-cooled lithium vanadium (SCLV) concept which builds on the ARIES-reversed-shear tokamak blanket concept (Tillack *et al.* 1997; Sze *et al.* 1998) and historic R&D activities at the Argonne National Laboratory Blanket program (Mattas *et al.* 1998; Gohar *et al.* 2000). The SCLV is embodied by the choice of a vanadium alloy (typically V-4Cr4Ti although advanced V alloys are also under development (Aaron Li 2024)) as structural material and pure lithium metal which serves as the breeder, coolant, multiplier and tritium carrier. An external multiplier and/or reflector may or may not be required depending on the design. Historically, lithium vanadium concepts have not been strongly considered for separate or dual-cooled designs because of concerns with oxidation and embrittlement by the uptake of interstitial atoms including oxygen, carbon, nitrogen or hydrogen (Muroga *et al.* 2014). However, both helium-cooled lithium vanadium (Lord *et al.* 2024) and dual coolant lithium vanadium (Li 2024) have been proposed recently, although these designs were not incorporated into this analysis due to time constraints and lack of sufficient technical detail.

The third is a self-cooled molten salt concept which is being developed by the Massachusetts Institute of Technology in collaboration with Commonwealth Fusion Systems (Sorbom *et al.* 2015; Ferry *et al.* 2023). This design builds on US blanket (Sze *et al.* 1986; Wong *et al.* 2005) and ITER program designs (Abdou *et al.* 2005), but with the major modification of removing flow channels and replacing them with a continuous pool of quasi-stagnant salt. This allows for the removal of a significant fraction of structural material for enhanced breeding performance, which historically was a challenge for molten salt concepts. The salt typically chosen for this application is FLiBe (2:1 molar mixture of LiF-BeF₂ salt eutectic) due to its lithium content and historical usage in the molten salt reactor experiment experiment at ORNL, which provides for a relatively robust operational baseline (Wong *et al.* 2005). This concept, known as the FLiBe liquid immersion blanket (F-LIB), initially proposes to utilize Inconel-718 as the structural material and Be as a neutron multiplier. It is important to note that Inconel-718 is not considered a low activation material due to its high nickel content, and so is not viable in the long term. However, it may be an acceptable choice for a low volume, one-of-a-kind plant assuming that suitable materials are identified and matured prior to full commercialization, which is an area of ongoing development (Commonwealth Fusion Systems 2024).

It should also be noted that several water-cooled designs were identified, but ultimately not explored. Although water cooling enjoys a relatively robust technology

basis, including application as a coolant in fossil and nuclear fission power plants, it was recognized that water-cooled systems have some significant challenges which limit their potential attractiveness for commercial DT fusion devices and ultimately were not an attractive pathway for the *FusionDirect* program. For a detailed discussion of these challenges, as well a perspective on why the US fusion program has not historically favored water as a coolant, readers are referred to Tillack *et al.* (2015).

The following sections of this paper detail the process by which each of the six blanket concepts were analyzed parametrically to better understand differences in performance. Section 3 details the neutronics analysis via Monte Carlo techniques, § 4 details the thermal analysis evaluating system-level integration and performance with a Rankine cycle and § 5 details a TFC analysis using the residence time method (RTM). In each of these sections, the associated tools were also used to evaluate the Infinity Two FPP baseline plasma physics configuration. Section 6 combines the outcomes of these quantitative analyses with a qualitative analysis of technical maturity and other performance risks and discusses implications of various blanket choices on the overall *FusionDirect* program. Section 7 details the conclusions of this study.

3. Neutronics analysis

3.1. Introduction

One of the most significant challenges in designing a stellarator-based fusion energy system is the selection of a blanket concept optimized for its complex geometry. From a large phase space of blanket concepts, a design and associated radial build must be chosen which is able to satisfy both tritium self-sufficiency and shielding requirements, constrained to as reasonably small build depth as possible in order to satisfy space limitations between the plasma and the magnets. For tritium self-sufficiency, the TBR must be greater than unity depending on the specifics of the TFC and objectives for doubling time. In the neutronics portion of this study, a TBR of 1.35 was set as the viability target, understanding that detailed system-level requirements have not yet been set, but also that significant margins may be necessary to accommodate additional fidelity in design details (El-Guebaly 2018). This includes detailed component geometries as well as the inclusion of the divertor, penetrations and gaps which will remove volume from the breeder layer. For shielding, conservative lifetime limits included: (i) restrictions on the fast neutron fluence at the magnets to below $5 \times 10^{18} \text{ n cm}^{-2}$ for super conductor degradation concerns (El-Guebaly 2018), (ii) He production/damage in the vacuum vessel below 1 atomic parts per million (appm) to ensure reweldability (El-Guebaly 2018) and (iii) 5 displacements per atom (dpa) as a conservative limit of radiation induced embrittlement of austenitic stainless steels (such as 304 and 316) used for the vacuum vessel (Zinkle & Was 2013). The target lifetime used in this study was five full-power years based on preliminary requirements and objectives of Infinity Two.

The body of this section details the approach for determining optimal radial builds for each family of breeder concepts using computational neutronic simulations, comparing the blanket concepts based on their optimal radial builds and arriving at the recommendation of the leading concept from a neutronics perspective. The radial build used for this analysis was based on the FNSF study (Kessel *et al.* 2018), excluding the blanket and magnets portions, which were drawn from the literature and T1E internal design activities, respectively. A key differentiator of this study with respect to other design activities was the decision to not allow water within the vacuum

boundary for engineering and safety considerations. This resulted in the creation of a water-cooled low-temperature shield as a layer external to the helium-cooled vacuum vessel which contains both the blanket and the high-temperature shield.

All neutronics simulations were performed using OpenMC (Romano *et al.* 2015) with FENDL 3.2c neutron cross-section data library, ENDF/B-VIII.0 supplement for Nd neutron and all element photon reaction cross-sections. The focus of the subsequent analysis sections is to outline the implication of blanket choices on radiation transport and subsequent effects, including neutron flux/shielding attenuation, tritium breeding, nuclear heating, material damage to blanket structures and He production by nuclear transmutation.

3.2. Parametric analysis of breeder blanket concepts

A simplified one-dimensional neutronics analysis was used to perform a comparative evaluation of six blanket concepts based on their breeding efficiency with breeder thickness, as well as the shielding efficiency with thickness of breeder and shield layers. These one-dimensional simulations were performed using a plasma ring source (Shimwell, 2021) and material-homogenized toroidal shell representations of the layers of interest (first wall, breeder, vacuum vessel, shielding, magnet coil winding pack, etc.). Although not fully representative of complex three-dimensional stellarator geometries, this type of simplified quantitative comparison is helpful to inform the down-selection of blanket concepts at early design stages (El-Guebaly *et al.* 2005, 2008). Models comprising concentric toroidal shells of homogenized blanket layers were generated based on the following references:

- a. HCPB (Zhou *et al.* 2023a), shown in figure 10 in Appendix A.
- b. HCLL (Aubert *et al.* 2018), shown in figure 11 in Appendix A.
- c. DCLL (Davis *et al.* 2018), shown in figure 12 in Appendix A.
- d. SCLL (Kessel *et al.* 2015), shown in figure 13 in Appendix A.
- e. SCLV (Gohar *et al.* 2000; Kirillov *et al.* 1998), shown in figure 14 in Appendix A.
- f. F-LIB (Segantin *et al.* 2020, 2022; Bae *et al.* 2022), shown in figure 15 in Appendix A.

The layers whose thickness were varied are denoted in the diagrams with turquoise for breeder layer and blue for shields. All other layers without ‘variable thickness’ designation in the diagrams were fixed in the parametric models. Toroidal shell models were parametrically generated for each blanket concept to cover the domain where the breeder thickness varies from 10 to 100 cm and the two shielding thicknesses vary from 10 to 60 cm.

For each breeder blanket concept, in addition to variation in breeder and shielding thickness, parametric studies were also performed to determine the variation in neutronic response for various relevant parameters including ^6Li enrichment, multiplier material and composition, composition of structural material and composition of coolant material. The reference cases listed in the previous section were used as a basis for comparison. In addition, for the HCPB concept the neutronic performance of several novel breeder materials of interest was also studied. Figure 1(a) shows the change in TBR and full-power year fast neutron fluence incident on the magnets with increasing breeder layer thickness and a shielding thickness of 10 cm for the

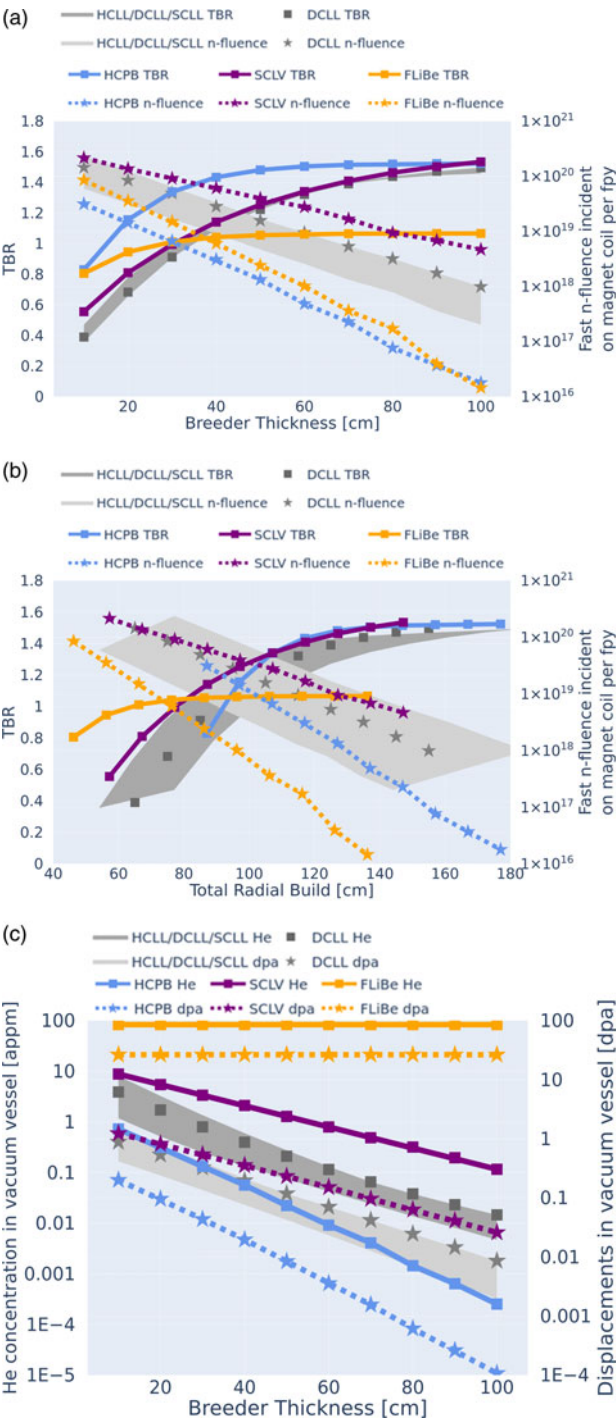


FIGURE 1. (a) The TBR and fast neutron fluence on the magnets vs homogenized breeder layer thickness. (b) The He concentration produced by transmutation in vacuum vessel per full-power year and dpa in vacuum vessel per full-power year vs breeder thickness. (c) The TBR and fast neutron fluence on the magnets vs radial build thickness reflecting that the blanket concepts differ in associated manifold sizes.

Blanket concept	Minimum breeder thickness ¹ (cm)	Associated total radial build (cm)	Associated configuration upper limit on TBR	He production in vacuum vessel per fpy less than 0.2 (appm)	Damage to vacuum vessel material per fpy less than 4 (dpa)
HCPB	50	127	1.46	Y	Y
HCLL	70	149	1.39	Y	Y
DCLL	90	145	1.47	Y	Y
SCLL	90	134	1.47	Y	Y
SCLV	100	147	1.47	Y	Y
F-LIB ²	60	96	1.06	N/A	N/A

¹Minimum breeder thickness that meets n-fluence limit on magnets approximately $1\text{E}18$ n/fpy.

²No shielding between first wall and vacuum vessel incorporated into design; this design concept is incompatible with vacuum vessel as lifetime component.

TABLE 3. Upper bound of tritium breeding performance for the blanket concepts of interest under standardized geometry and the minimum shielding needed to meet magnet and vacuum vessel lifetime requirements.

high-temperature shield and low-temperature shield, which is the minimum shielding in the cases studied. Figure 1(b) shows the same TBR and fast neutron fluence incident on magnets with increasing breeder thickness as in figure 1(a), but with respect to total radial build to reflect the fact that different breeder concepts differ in associated manifold sizes and support structures. Figure 1(c) shows He production and damage in the vacuum vessel with increasing breeder layer thickness. In figure 1(c) the concentration of He in the vacuum vessel material in appm was calculated from the He production tally in the vacuum vessel normalized to the atomic number density of material in the cell volume. The expected dpa in the vacuum vessel material was calculated from the mean damage energy tally in Fe for cases where the vacuum vessel material is steel (for the blanket concepts HCPB, DCLL, HCLL, SCLL); in vanadium, titanium and chromium for cases where the vacuum vessel material is V-4Ti-4Cr (SCLV); in nickel, iron and chromium, for cases where the vacuum vessel material is Inconel 718 (F-LIB). Data reduction was performed according to the following heuristic: the minimum breeder thickness was determined for each blanket concept for 10 cm each of high-temperature and low-temperature shielding which meets the magnet shielding constraints of less than 1×10^{18} n cm⁻² per full-power year. The associated TBR was noted as well as whether this radial build satisfies vacuum vessel damage constraints. The results of this data reduction are listed in table 3. In this way the blanket concepts can be compared simultaneously on 3 axes: compactness of radial build, TBR and shielding.

These results indicate that the HCPB concept promises a very high upper bound TBR of 1.46 for a relatively mid-sized radial build, presenting a compromise between high tritium breeding performance and compact radial build. In addition, it is evident that the HCPB concept saturates at almost the highest TBR with the lowest breeder material loading. Finally, it is clear that solid ceramic breeder materials afford the greatest supplemental shielding effect to both the vacuum vessel and magnets for the most compact radial build, which benefits the economics of the TIE design in both minimizing the size and maximizing the lifetime of the device by minimizing the damage on lifetime components. This performance can be attributed to the higher atomic number density of the solid breeder materials even in the case of

a pebble-based design, as well as the utilization of Be-based materials for highly effective neutron multiplication.

The breeding and shielding with material thickness of the DCLL was found to be intermediate between the SCLL and HCLL. This is expected because the DCLL supplements He cooling with PbLi cooling to offset some of the He manifold thickness resulting in a more compact radial build than the HCLL but not quite as compact as the SCLL. On the other hand, the DCLL exhibits a higher TBR than the HCLL as expected due to the higher PbLi mass loading in the device. Of all liquid PbLi concepts, the SCLL is by far the most compact and tritium breeding-efficient. From [figure 1](#) and [table 3](#), it can be seen that the PbLi designs and SCLV promise the highest saturated TBR (approximately 1.47), but also have the highest associated total radial build requirements, with their performance being comparable. The key difference between these concepts is the requirement for ^6Li enrichment, where the pure lithium holds a clear advantage by utilizing natural enrichment versus the 90 % enrichment utilized by the PbLi concepts. The large radial builds required for the liquid metal concepts can be attributed to the lower moderation and multiplication efficacy of liquid metals, which negatively impacts both breeding and shielding performance.

[Figure 1](#) and [table 3](#) show that the F-LIB concept achieves a TBR greater than unity at the smallest radial builds, but it also saturates at lower values (1.09) and ultimately is the only concept which fails to meet the target TBR of 1.35. Regarding shielding, it is evident that the F-LIB concept provides the greatest shielding to the magnets thanks to the high neutron moderating and absorbing properties of FLiBe constituent nuclides, although it is this shielding capability that ultimately limits the saturated TBR due to self-shielding effects. These findings are consistent with prior neutronics studies of the F-LIB (Segantin *et al.* 2020), and although opportunities exist for refinement and potential improvement of the TBR in FLiBe-based blankets through the careful tailoring of ^6Li enrichment, multiplier content and detailed layout (Segantin *et al.* 2020; Boullon *et al.* 2021), such optimizations were outside the scope of this study. In addition, the F-LIB concept is not conceived with the intention of the vacuum vessel being a lifetime component, which explains why its design precludes any substantial shielding of the vacuum vessel and neutron fluence is permitted to exceed material damage limits. Finally, it should be noted that this particular reference design assumed zero structure in the blanket, which is not currently envisioned as being applicable to the T1E high-field stellarator approach. This is due to specific design decisions which require structural elements for supporting the vacuum vessel, tank sector separators for modularity and penetrations for plasma access. In addition to the lowest saturated TBR, the F-LIB concept was also found to be sensitive to this additional structure requirement which negatively impacts the TBR.

As a supplement to the reference configurations above, a wide variety of neutronics calculations in simplified geometric approximations were performed to better probe and understand the overall design space for breeder concepts consistent with prior studies (Zheng & Wu 2003), but using modern tools and more representative geometries. One such example is shown in [figure 2](#), where the TBR was calculated for various breeder materials mixed homogeneously with concentrations of multiplier (Be_{12}Ti) increasing in the y -direction. The relationship between breeder thickness and TBR was then calculated at enrichments increasing in the x -direction and with varying multiplier material content in the breeder region. This analysis

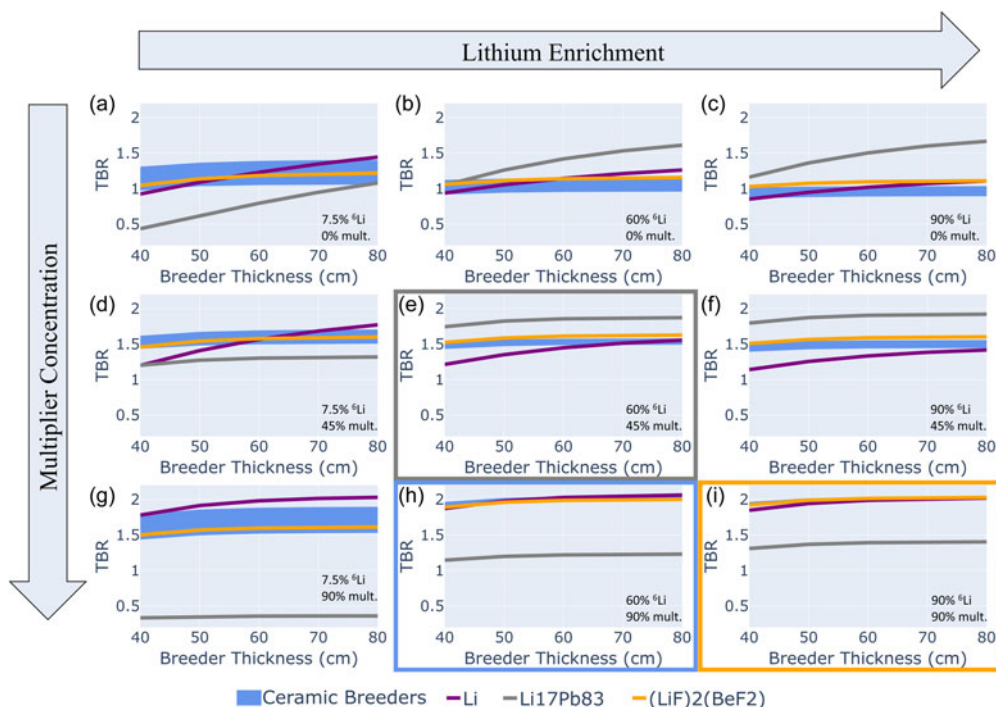


FIGURE 2. Relationships of breeder thickness and TBR using (a) natural lithium without multiplying material, (b) 60 wt % ^6Li enrichment without multiplying material, (c) 90 wt % ^6Li enrichment without multiplying material, (d) natural lithium with 45 wt % multiplying material, (e) 60 wt % ^6Li enrichment with 45 wt % multiplying material, (f) 90 wt % ^6Li enrichment with 45 wt % multiplying material, (g) natural lithium with 90 wt % multiplying material, (h) 60 wt % ^6Li enrichment with 90 wt % multiplying material and (i) 90 wt % ^6Li enrichment with 90 wt % multiplying material. For the three ceramic breeder materials of interest, the blue shaded regions show the maximum TBR for the lowest resource utilization.

enables a comparison of breeder materials from the point of view of resource utilization, where designs utilizing low ^6Li enrichment and low Be multiplier loading are most desirable, although the detailed optimization of engineering, safety and cost trade-off between these two aspects is still an open question requiring resolution. The compactness of the radial build is reflected by the breeder thickness as a proxy.

The superiority of solid breeder materials Li_2O , Li_4SiO_4 and Li_2TiO_3 is highlighted by figure 2(d) where compact radial builds with breeder thicknesses as low as 50 cm, multiplier concentration as low as 45 weight percent (wt %) and ^6Li enrichment as low as natural ^6Li abundance can achieve TBR approximately 1.6, the highest of all materials. Using natural lithium and less than 45 wt % of multiplying material mixed with the breeder material, Li_2O generally outperformed the other breeding materials up to thicknesses of 70 cm. The TBR calculated using natural liquid lithium was slightly higher than Li_2O when using a 90 wt % composition of multiplying material. At low lithium enrichments and low multiplying material content, Li_2O has the highest TBR at depths relevant to T1E designs and implies a potential pathway for a natural lithium blanket beyond pure lithium metal.

The color-coded boxes show the maximum TBR for the lowest resource utilization for three breeder materials of interest: [figure 2\(e\)](#) was identified as the case showing the best TBR for liquid lead-lithium (gray), [figure 2\(i\)](#) was identified as the case showing the best TBR for FLiBe (yellow) and [figure 2\(h\)](#) was identified as the case showing the best TBR for Li_2O , Li_4SiO_4 and Li_2TiO_3 (blue). In this representation it becomes clear that liquid PbLi offers the highest TBR for the lowest absolute resource utilization of all cases of interest which highlights the attractiveness of the breeder material. It is also the breeder that performs the best in scenarios where only ^6Li enrichment is employed ([figures 2b](#) and [2c](#)). FLiBe only offers superior TBR with maximum resource utilization; however, it is possible for FLiBe to achieve a TBR greater than unity with only natural ^6Li if the ‘compact radial build’ constraint was relaxed. In these circumstances, the TBR can benefit from elevated ^7Li reactions with increased moderation deeper into the FLiBe breeder material for increased ^6Li reactions.

The results of these studies using simplified approximations illustrate the parameter space for different breeding media and understand opportunities in nuclear design for breeder blankets. In general, it was found that solid breeders have the best, most well-rounded performance in regions of interest. PbLi was found to be the best breeder for scenarios where Be multiplier is undesirable. Similarly, pure lithium is the most apparent candidate for scenarios where ^6Li enrichment is undesirable, although opportunities exist for other breeders with proper optimization. Finally, FLiBe is the leading candidate for circumstances where shielding efficiency is a primary consideration.

3.3. Detailed three-dimensional analysis of paraStell models

This section discusses the application of the T1E automated space-claim algorithm to virtually build out non-uniform stellarator blanket structures for a given plasma configuration. This tool is being developed for the optimization of TBR constrained by shielding to meet lifetime needs. Additionally, it enables analysis of spatially resolved neutronics responses in various blanket structures for a given plasma configuration, including identification of regions most vulnerable to neutron damage. Given resource limitations, only the HCPB and DCLL blanket concepts were examined using these higher fidelity tools.

This three-dimensional neutronics analysis made use of ParaStell, which is an open-source python code developed by Moreno *et al.* (2024) to automate the parametric computer-aided design (CAD) geometry generation of stellarator blanket structures with uniform thickness given the geometrical definition of the plasma, in this case, the Infinity Two configuration. As part of the workflow for the three-dimensional neutron transport simulations, the first step is to simulate the plasma as a volumetric neutron source with full fidelity of the distribution of DT reaction density in space ([figure 3a](#)). This three-dimensional neutron source is used to derive the two-dimensional spatial distribution of 14.1 MeV neutron flux on the first wall, i.e. neutron wall loading (NWL) ([figure 3b](#)).

It is evident that the radial distance normal from the stellarator first wall to the nearest bounding magnet is not uniform over the field period ([figure 3c](#)). This means that blanket structure thickness can be optimized according to the neutron flux and available space in every radial direction. An optimized blanket build potentially has non-uniform breeder and shield thicknesses. The second step therefore is to obtain a matrix representing the radial distances between the last closed flux surface of

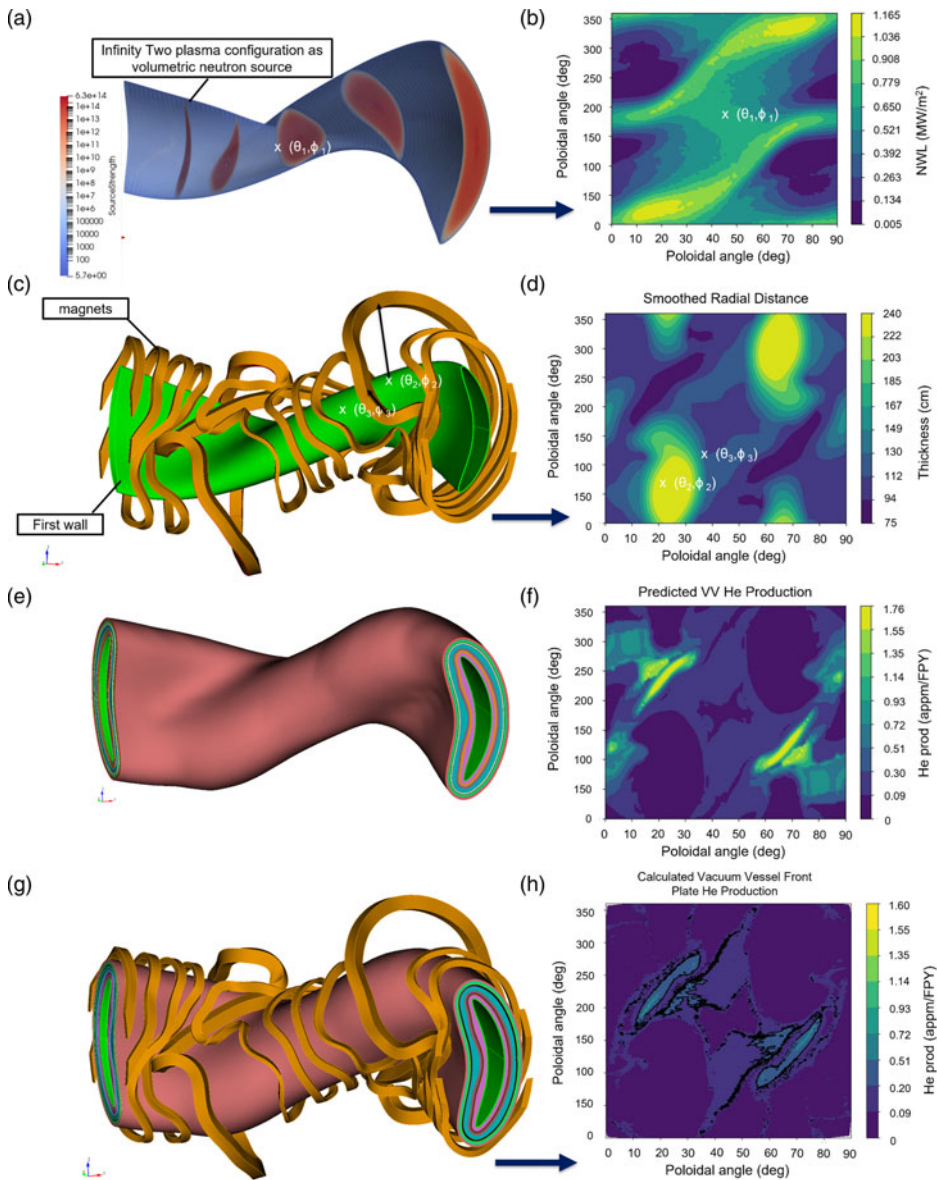


FIGURE 3. (a) Three-dimensional representation of neutron density of the Infinity Two plasma modeled as a volumetric neutron source. (b) Two-dimensional projection of the loading of neutron flux on the first wall due to neutron production from the plasma as a DT neutron source in units of MW/m^2 . (c) Three-dimensional CAD of the first wall based on Infinity Two geometry and its relevant magnets. (d) Output from radial distance finder algorithm: two-dimensional projection of radial space for building structures. (e) Three-dimensional CAD of the blanket structures automatically built out given the radial build space shown in figure 1(d). (f) An example of the He production in the vacuum vessel in this stellarator build predicted by the index. (g) Three-dimensional CAD of geometry definitions of blanket structures with magnets imported into OpenMC for neutronic simulations. (h) He production in the vacuum vessel in this stellarator buildout determined by neutronic simulations of the geometry in (g).

the plasma and the magnets (figure 3d). A proprietary tool was developed for this purpose.

The third step is to optimally allocate the available build space in each radial direction between breeder and shielding material and generate the geometry for every associated layer, as shown in figure 3(e). Figure 3(f) shows the first-order expected neutronic performance on one metric of interest based on this optimization, in this case for example He production by neutron-induced transmutation in the vacuum vessel. This first-order prediction is based on the index of neutronics responses in the relevant blanket build collated from the one-dimensional parametric neutronics study. The one-dimensional radial build configurations for each blanket concept collated are provided in Appendix A.

The blanket layer geometries are then combined with the magnet coil geometries as a full field period of the stellarator geometry (figure 3g) for full neutronics simulations with OpenMC. Figure 3(h) shows the actual neutronics performance of this geometric model according to the simulation for the same metric – He production in vacuum vessel. The spatial distribution of He-production hotspots predicted in figure 3(f) accurately reflects the distribution obtained in the full simulation.

The radial build space available for the Infinity Two configuration and coil set is shown in figure 3(d), with brighter regions indicating where in toroidal, poloidal space the magnets afford a wider berth for the potential insertion of more breeder or shielding material. The available radial build distance map is dictated only by plasma configuration and coil set, and is therefore independent of the blanket concept. The NWL response matrix (figure 3b) dictates the net shielding on the magnets required, thereby informing the assignment of breeder, high-temperature shield and low-temperature shield thicknesses constrained by radial build space (figure 3d). The radial build layers for HCPB are shown in Appendix A, figure 10 and the radial build layers for DCLL are shown in Appendix A, figure 12. The primary difference between the HCPB layers and DCLL layers outside of breeder layer compositions (including breeder material, multiplier and structural materials) and its back wall (abbreviated ‘bw’ in the diagram) are the size of the manifold: the HCPB reference concept was designed for the manifold layer to scale with the breeder layer; the DCLL reference concept was designed for a uniform manifold layer, with radial thickness of 6 cm.

The automated radial build algorithm resulted in the HCPB requiring a much thinner maximum radial build, reflected in the predominance of cooler hues in the color scale plot in the HCPB compared with DCLL, in figures 4(a) and 4(b). The algorithm assigned the HCPB a maximum breeder thickness of 143 cm (figure 4a) to achieve TBR greater than 1 (unity) compared with the DCLL, which was assigned a maximum breeder thickness of 184 cm (figure 4b) for similar results, both with comparable shielding. This represents the first major advantage of the HCPB concept over the DCLL concept in that a lower volume of breeder medium is required to achieve a superior TBR. However, it should be noted that the excess balance in the HCPB radial build was not assigned to breeder, high-temperature shield or low-temperature shield and instead was assigned as a manifold layer, which highlights a potential weakness of the HCPB concept which will be further investigated during detailed design activities. The second major advantage of the HCPB concept reflected in the models is that the resulting algorithmic build-out shows a shield

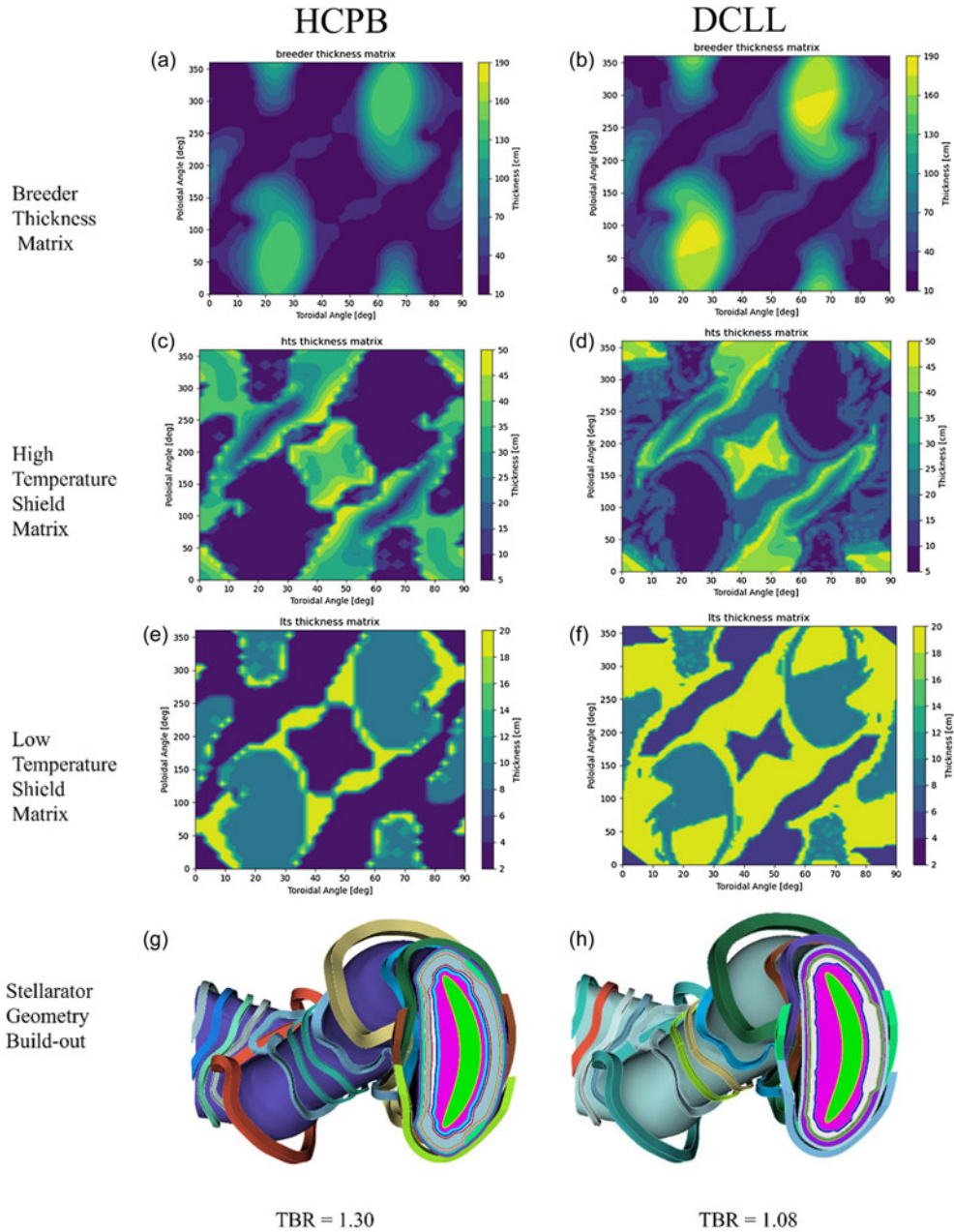


FIGURE 4. (a) Breeder thickness matrix in (θ, ϕ) , HCPB; (b) breeder thickness matrix in (θ, ϕ) , DCLL; (c) high-temperature shield thickness matrix in (θ, ϕ) , HCPB; (d) high-temperature shield thickness matrix in (θ, ϕ) , DCLL; (e) low-temperature shield thickness matrix in (θ, ϕ) , HCPB; (f) low-temperature shield thickness matrix in (θ, ϕ) , DCLL; (g) ParaStell geometry generated for HCPB layers; (h) ParaStell geometry generated for DCLL layers.

design with far fewer contours for the HCPB – which is very desirable for ease of manufacturability – compared with the more DCLL shield design which shows widespread ripple-like contours. This effect is most evident in the high-temperature shields (figures 4c and 4d). The required low-temperature shield thickness is lower on average for the HCPB with predominance of cooler colors in the low-temperature shield thickness matrix (figure 4e) as compared with the one for DCLL (figure 4f).

The result of this automated buildout is represented by figure 4(g) for HCPB and figure 4(h) for DCLL. The difference in breeder material (pink layer in figures 4g and 4h) thickness required for each build for HCPB and DCLL is readily apparent: the DCLL requires a greater breeder material thickness than the HCPB. OpenMC neutronic simulations run with 300 M particles found the TBR for the HCPB case to be 1.30 and the DCLL case to be 1.08. These TBR results are deemed satisfactory at this stage given the level of fidelity as well as the results of § 5 and the various opportunities for continued improvement with subsequent iterations.

The combination of varying NWL and radial build thickness of the breeder/shielding layers leads to the expectation that damage primarily occurs in highly localized regions of the various components of interest. The T1E high-throughput workflow enables rapid identification of the presence and location of these high-damage regions for any given plasma–magnet configuration which feeds back into the overall stellarator optimization workflow. To illustrate this point, figure 5(a) shows the mapping of the neutron fluence on the magnet regions in toroidal, poloidal coordinates, which can be rapidly produced without the need for time and computationally intensive three-dimensional neutronics. The blank zones in figure 5(a) reflect regions where predicted neutron fluence is so low that they fall outside the bounds of the developed neutronics response index. Compared with the full stellarator geometry simulation run over seven days on a high-performance computing cluster shown in figure 5(b), the rapid mapping has correctly identified the regions in which the neutron fluence limits are violated at greater than $1 \times 10^{18} \text{ n cm}^{-2}$ per full-power year (green and warmer colors) to a first-order level of accuracy. A three-dimensional representation of the spatial distribution of fast neutron fluence on the magnets is shown in figure 5(c). White and blue regions indicate where the fluence on the magnets meet design constraints of less than or equal to $1 \times 10^{18} \text{ n cm}^{-2}$ per full-power year and red regions indicate where this constraint is violated with greater than $1 \times 10^{18} \text{ n cm}^{-2}$ per full-power year. Figure 5(c) generally reflects that hotspots are predicted mostly on the inboard side.

At this juncture, it must be emphasized that the results presented here are for a simplified neutronics model of an early design iteration and do not constitute a final, optimized radial build at full engineering fidelity. The current radial build model is a high-level placeholder for use in an initial scoping analysis, and it will be refined to incorporate opportunities for reduced component volumes and increased shielding performance moving forward. In addition, the radiation limits on lifetime components are dependent on design and in some cases are not based on quantities which are well understood, such as the radiation limits on high-temperature superconducting magnets (Unterrainer *et al.* 2022). As such, they are subject to modification as both fundamental understanding and design fidelity improves. Given these points, the current findings show that the Infinity Two configuration has sufficient performance and no fundamental roadblocks exist towards the continued optimization of radial builds which will satisfy detailed performance and engineering requirements.

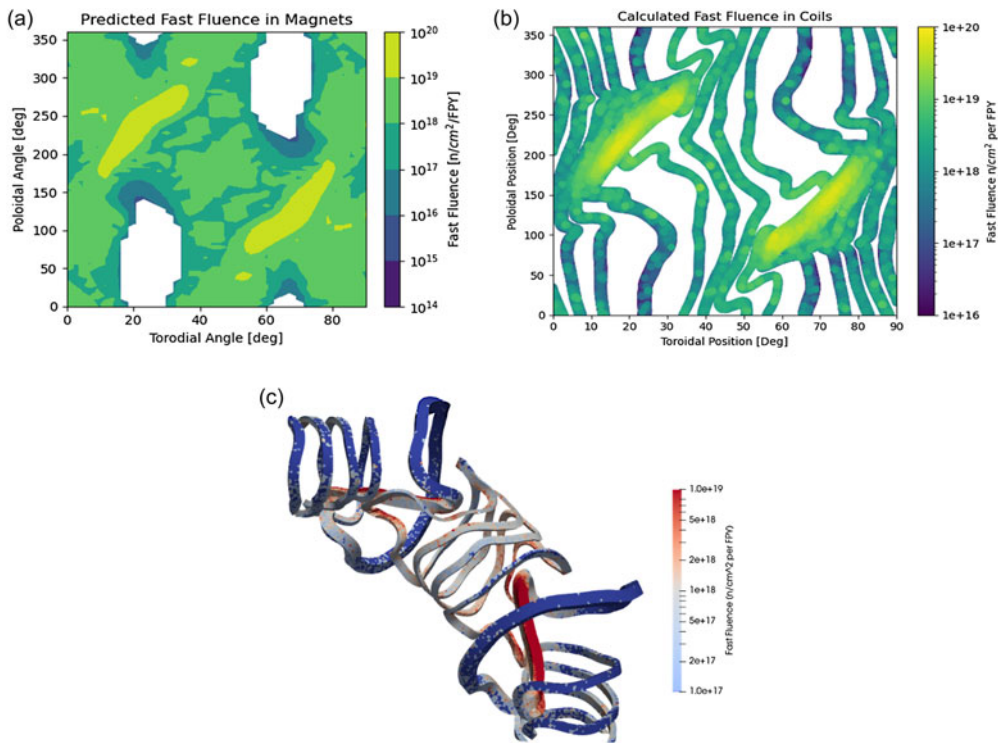


FIGURE 5. (a) Two-dimensional spatial distribution of neutron fluence per full-power year at magnet locations in (θ, ϕ) predicted based on neutronics response index generated from the rapid optimization workflow step 2 for HCPB radial build configuration. (b) Two-dimensional spatial distribution of neutron fluence per full-power year at magnet locations in (θ, ϕ) based on full stellarator geometry simulation of HCPB radial build configuration. (c) Three-dimensional representation of space-resolved neutron fluence per full-power year on stellarator magnets based on full stellarator geometry simulation of HCPB radial build configuration.

4. Thermal analysis

4.1. Introduction

This section presents a sensitivity analysis of the various blanket concepts and their possible integration with a Rankine thermodynamic cycle, which was selected as the baseline due in large part to its robust industrial base and existing supply chain. The primary focus of this study was to understand the potential of each concept for producing at least 100 MW_e as a nominal minimum target for Infinity Two. To ensure flexibility in design space and allow operation over a range of fusion plasma power, a fusion plasma power of $400 \text{ MW}_{\text{th}}$ was used as the low-end baseline for evaluating this performance. The scalability of these results was also explored for designs up to $1000 \text{ MW}_{\text{th}}$ of fusion plasma power. The blanket concepts and baseline design parameters evaluated in this study are listed in [table 4](#).

In an MFE energy system, heat is distributed throughout the power core and high-grade heat sources typically include the blanket, the divertor and potentially the vacuum vessel, depending on design. For this analysis, only the blanket and divertor were considered as heat sources, with the assumption that all heat not directed at the

Reactor loop ¹	HCPB	HCLL	DCLL		SCLL	SCLV	F-LIB
Fusion plasma power (MW)	400	400	400		400	400	400
Multiplication factor	1.3	1.15	1.15		1.1	1.1	1.2
Thermal power (MW)	506	458	458		442	442	474
Coolant	He	He	PbLi	He	PbLi	Li	FLiBe
T_{in} (°C)	300 (350)	300 (350)	300 (350)	350 (350)	500 (700)	500 (500)	530 (500)
T_{out} (°C)	500 (600)	500 (600)	500 (700)	475 (500)	700 (1050)	600 (700)	630 (700)
Mass flow (kg/s)	366 (293)	331 (265)	3565 (2852)	322 (268)	8799 (5028)	789 (295)	1482 (741)
Divertor T_{in}/T_{out} (°C)	500/600	500/600	500/600	(600/700)	600/700 (900/1000)	600/700	530/630
Divertor mass flow (kg/s)	244	221	221		213	213	494
Pressure drop (MPa)	0.26	0.56	2.0		0.25	0.064	1.0
Pumping power (MW)	8.76 (7.62)	17.5 (15.2)	0.83 (0.49)	12.6 (10.7)	0.24 (0.15)	0.08 (0.03)	0.47 (0.23)
Intermediate loop ¹							
Mass flow (kg/s)	365 (292)	330 (264)	180 (268)		320 (183)	640 (320)	910 (343)
T_{in} , I-blanket HX (°C)	250 (287)	250 (287)	238 (463)	319 (313)	450 (612)	475 (450)	505 (450)
T_{out} , I-blanket HX (°C)	450 (538)	450 (538)	319 (560)	444 (463)	650 (961)	575 (650)	605 (650)
Pumping power (MW)	4.88 (4.17)	4.42 (3.78)	2.48 (6.28)		6.11 (4.26)	12.7 (10.3)	18.7 (6.55)

¹Values in each cell are for the basic concepts. Values in parentheses are for the advanced concepts.

TABLE 4. Summarized thermal parameters for blanket concepts under consideration.

divertor (conservatively assumed to be 25 %) is instead deposited in the blanket. In the case of the F-LIB concept, the internal vacuum vessel is cooled with molten salt which is discharged directly into the blanket and keeps in convention with this same assumption. In addition to the heat being deposited in the blanket, each concept has an additional neutron energy multiplication factor, which for the purposes of this study were assumed to be the same as those developed by El-Guebaly *et al.* (2005). This energy multiplication factor results in a different total thermal power for each blanket concept, assuming a standard fusion plasma power.

The pressure drops shown in table 4 are based on values found in the literature for each reference design (Sagara *et al.* 1997; Gohar *et al.* 2000; Giancarli *et al.* 2002; Hernández *et al.* 2017; Aubert *et al.* 2018; Smolentsev *et al.* 2018). The pumping power of each blanket concept was then calculated using the mass flow rate of the blanket and divertor using the assumed pressure drop from the literature. An isentropic efficiency of 100 % was assumed for all pumps/compressors used in the blanket loop given the variety of coolants used. Since the pressure drop is highly dependent on design specifics, it was varied parametrically to calculate the required pumping power and thus efficiency of each concept in this analysis across a range of potential values. Similarly, the operating temperatures, both high end and low end,

are primarily dictated by the structural material of choice and compatibility with applicable coolants (Zinkle & Ghoniem 2000). In the case of the DCLL, the helium temperature range is not consistent throughout literature. For this reason, the helium temperature range in the DCLL was based on a similar temperature change but within the temperature range used in the references. The initial temperature ranges, as well as associated parameters like mass flow and pumping power, are shown in [table 4](#) and are based on the baseline assumption for structural materials. If advanced materials become available, it is possible to broaden the temperature window of all the blankets concepts to improve overall performance (Zinkle & Ghoniem 2000). The second value in columns with multiple values in [table 4](#) shows the parameters associated with designs which use these advanced materials. One point of note is that the SCLL only has an advanced design utilizing SiC composites, but in order to provide an additional comparison point between concepts a lower-temperature SCLL was run consistent with the SCLV advanced parameters, which are the values shown for the SCLL baseline configuration in [table 4](#).

For this analysis, an intermediate heat transfer system using He was implemented between the primary loop and the Rankine cycle loop for all blanket concepts. The parameters for these intermediate loops are shown in the intermediate loop section of [table 4](#). The intermediate loop serves as a barrier separating the water in the Rankine loop from the breeder in the blanket loop, which may contain tritium and liquid lithium-based coolants, depending on the concept. These liquid lithium-based coolants can have strong reactions to water at elevated temperatures, which could potentially lead to exothermic reactions and/or explosivity, and the intermediate loop helps to prevent such interactions. It also helps to avoid the creation of tritiated water. Both phenomena have safety and economic implications and for these reasons, gaseous, relatively inert coolants like He or CO₂ are considered for the intermediate loop. Other types of coolants such as molten salts have been considered for the same reasons above, with the benefit of serving in a thermal storage capacity which is important for pulsed concepts such as the tokamak (Barucca *et al.* 2021). Some concepts like the HCPB do not necessarily require an intermediate loop, but an intermediate loop was assumed as a baseline for all concepts to better compare performance under equitable conditions. An analysis without an intermediate loop was also performed for the relevant concepts and is discussed further in § 4.3.

For the power loop, a Rankine cycle with reheat was analyzed. The temperature-entropy (T-S) diagram and the cycle configuration are shown in [figure 17](#) in [Appendix A](#). In this configuration, the blanket heat is deposited in the intermediate loop and used to create superheated steam in the Rankine cycle loop. The diverter heat is used to reheat the steam in the Rankine side. A temperature difference of 100 °C between the maximum intermediate loop temperature and the inlet turbine temperature was assumed. Other assumptions include an isentropic efficiency of 0.85 for both the pump and the turbine. The steam quality at the turbine outlet was set to 0.90 for the lower-temperature end pressure cycles and to 0.99 for the higher-temperature end pressure cycles. A pressure drop of 0.5 MPa was used for every heat exchanger. Recirculating power for auxiliary systems, plasma heating and other sources of pressure drop apart from the pressure drop in the blanket loop were not considered in the analysis.

A python script was developed to perform the parametric analysis capable of calculating how the mass flow rate, net power and efficiency changed with varying conditions like blanket pressure drop, fusion power, steam quality, etc. using the

energy balance equation. The IAPWS R 7–97(2012) python module was used to calculate all the thermodynamic states of steam in the Rankine cycle loop. The module requires two initial parameters (pressure, temperature, entropy, enthalpy or steam quality) to return the remaining thermodynamic parameters needed.

4.2. Intermediate loop and blanket pressure drop analysis

An analysis of the primary blanket heat exchanger between the blanket and the intermediate loop was performed to understand performance discrepancies between concepts. The outlet temperature of the blanket/intermediate heat exchanger shown in [table 4](#) was calculated using the effectiveness-number of transfer units (ϵ -NTUs) method. As shown in [table 4](#), the DCLL blanket requires the smallest intermediate coolant mass flow rate due to the usage of dual coolants and heat exchangers for the transfer of heat to the intermediate loop. Since the heat is divided across two different coolants (46% of the heat removed by He and the rest by PbLi (Wang *et al.* 2015)), the heat capacity rate of the PbLi is the smallest out of all the analyzed designs, meaning that it is more suitable for transferring heat. The end result is that less intermediate coolant is needed to extract heat in the PbLi heat exchanger. The He heat exchanger is then used to further heat the intermediate coolant after the PbLi heat exchanger. Although the SCLL is also cooled by PbLi, its blanket mass flow rate is almost double that of the DCLL resulting in a higher heat capacity rate than the DCLL. As a result, the SCLL requires approximately twice as much intermediate coolant as the DCLL. The HCPB, HCLL and SCLL all have similar heat capacity rates leading to similar intermediate coolant mass flow rates. In contrast, the SCLV and FLiBe blanket will require the largest intermediate loop, as they need the most intermediate coolant due to their higher heat capacity rate.

In addition to the intermediate loop, one of the main factors that affects net power is the power required to pump the coolant through the blanket, which is an identified challenge for fusion power devices and has been a subject of study (Sagara *et al.* 1997; Gohar *et al.* 2000; Giancarli *et al.* 2002; Hernández *et al.* 2017; Smolentsev *et al.* 2018; Aubert *et al.* 2018). Specifically, MHD effects are one of the biggest factors to consider in liquid metals since it can induce a significant pressure drop in high-field MFE systems, and it remains a phenomenon that is not well understood (Smolentsev 2021). Given that the pressure drop in a stellarator may be highly configuration dependent, the pressure drop was varied when calculating the pumping power, with the purpose of comparing blanket designs and its potential impact on overall system efficiency. The pressure drop range was chosen with the recognition that the total pressure drop in the primary blanket loop is not limited to just the pressure drop in the blanket, and that ancillary equipment, including the tritium extraction system and the primary coolant/intermediate heat exchanger may contribute to a larger aggregate pressure drop. According to Smolentsev *et al.* (2018), this pressure drop could be comparable to or even exceed the MHD pressure drop in a DCLL blanket, with rough estimates suggesting that the sum of individual pressure drops in the ancillary system could be up to approximately 2 MPa. The pressure drop range explored in this analysis was between 0.05 and 4 MPa for all the blanket concepts. This broad range represents reasonable limits on allowable pumping power for the liquid-cooled concepts. It should be noted that the allowable pressure drop limits for He are much narrower than for the liquid concepts. The pumping power was calculated using density for the liquids, which were assumed to be incompressible, and enthalpies for He.

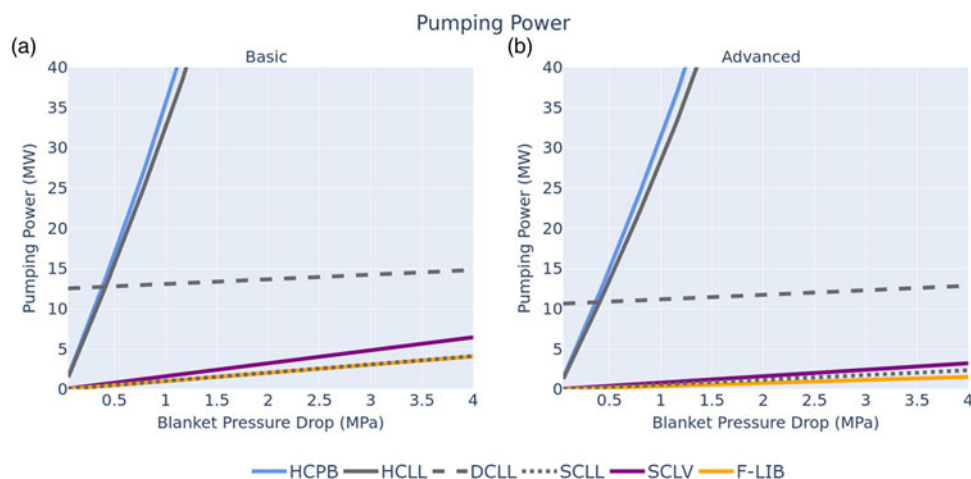


FIGURE 6. Pumping power comparison for the (a) basic concepts and (b) advanced concepts.

A comparison of pumping power for the baseline blanket concepts can be seen in [figure 6\(a\)](#). The results show that the He-cooled blankets both require the highest pumping power and are more sensitive to pressure drops. Even though both the HCPB and HCLL blankets have the same coolant and coolant temperatures, the HCPB has higher pumping power than the HCLL due to its higher energy multiplication factor, which results in higher thermal power and subsequently a higher mass flow rate and associated pumping power. For the DCLL, only the pumping power of PbLi was varied, and a constant pressure drop of 0.39 MPa was assumed for He ([Melichar *et al.* 2017](#)). The pumping power of He was calculated using this pressure drop and added to the pumping power of PbLi in order to calculate the total pressure drop for the DCLL concept. Results show that the DCLL concept requires the most pumping power out of all the non-He-only blankets, due to the relatively large pumping power required for He.

A comparison of pumping powers for the advanced blanket concepts with expanded operating temperatures can be seen in [figure 6\(b\)](#). Increasing the temperature range reduces mass flow rate by a factor of approximately two for all the blanket concepts, which results in an analogous drop in pumping power. The advanced He-cooled blankets are still the most sensitive to pressure drop, and the DCLL requires the highest pumping power compared with the other non-He blankets. The SCLV and the SCLL have similar pumping powers, and F-LIB requires the least pumping power, consistent with the basic designs. It should be noted that the assumed pressure drops stayed constant across the analysis of both the basic and advanced designs. However, because the coolant velocities and temperature differences shift rather substantially compared with the basic blanket concepts, it is expected that different pressure drops will vary between concepts. This discrepancy in pressure drop was not accounted for in this study and requires further analysis in future work. Finally, it should be noted that even the highest pumping power values shown in [figure 6](#) are below 5% of the total power for the liquid-cooled blanket concepts, which is a general limit on targeted pumping power percentage presented in the literature and the one used for this analysis. For the helium-cooled blankets (HCPB and HCLL) a pumping

Power loop ¹	HCPB	HCLL	DCLL	SCLL	SCLV	F-LIB
Turbine inlet temperature (°C)	358 (438)	356 (437)	356 (466)	549 (763)	475 (550)	480 (524)
Reheat temperature (°C)	422 (575)	410 (549)	452 (638)	689 (992)	660 (684)	602 (648)
Turbine inlet pressure (MPa)	14 (15)	14 (15)	14 (18)	18 (20)	16 (18)	16 (18)
Work turbine (MW)	177 (213)	163 (197)	160 (200)	203 (251)	181 (203)	201 (210)
Total pumping power (MW)	18.3 (16.4)	26.4 (23.3)	16.3 (20.7)	10.3 (8.50)	16.8 (10.3)	21.1 (8.46)
Net power (MW)	159 (190)	136 (173)	144 (180)	193 (243)	165 (193)	180 (202)
Rankine efficiency (%)	34.2 (40.2)	33.5 (42.8)	36.4 (43.1)	45.6 (54.2)	40.6 (45.5)	42.1 (44.3)
Net efficiency (%)	29.9 (37.4)	28.4 (36.2)	33.7 (39.5)	43.6 (53.7)	37.1 (42.3)	37.9 (42.9)

¹ Values in each cell are for the basic concepts. Values in parentheses are for the advanced concepts.

TABLE 5. Summarized parameters of Rankine cycle loop with reheat assuming the pressure drop from [table 4](#).

power of less than 5 % total power is achieved with a pressure drop of less than 0.77 MPa.

4.3. Power cycle sensitivity analysis

[Figure 7](#) shows the net power and efficiency results for the reheat cycles of the various blanket concepts, with the individual designs shown in [table 5](#). [Figure 7\(b\)](#) indicates that all of the basic blanket concepts can achieve efficiencies higher than 30 % so long as the primary loop pressure drops are kept below the most extreme values. For the HCPB and HCLL, 30 % efficiency is obtained when the pressure drop is below 0.24 MPa. The SCLL blanket concept is the only basic concept which achieves efficiency greater than 40 %, while the SCLV and F-LIB achieve efficiencies in the range of 35 %–40 %. The three low-temperature concepts all have efficiencies in the range of 30 %–35 % due to the utilization of similar, lower operating temperature structural materials, as well as He coolant, which results in comparable pumping powers. Of the three, the HCPB achieves the highest net power due to its higher energy multiplication factor in the blanket. When an intermediate loop is not included for the baseline HCPB and HCLL, both the net power and the efficiency increase by approximately 10 %. This is due to the net pumping power being significantly lower, as the intermediate loop requires a relatively high He mass flow rate and additional heat exchangers which lead to pressure drop, resulting in non-trivial additional pumping power. In addition, the elimination of the intermediate loop allows for higher inlet turbine temperatures in the Rankine cycle, which boosts efficiency.

The net power and efficiency for the advanced blanket concepts were also analyzed and the results, indicated in the parentheses, can be found in [table 5](#) as well as illustrated in [figures 7\(c\)](#) and [7\(d\)](#). With the advanced concepts, both the outlet temperature and temperature difference are higher. As shown in the pressure drop analysis, having a higher temperature difference leads to a lower mass flow rate for a given fusion power, resulting in a lower pressure drop curve. As expected, the net power and efficiency increase rather significantly for all concepts. The efficiency of the lower-temperature blankets (HCPB, HCLL, DCLL) increased by 7 %. The SCLV and F-LIB concepts also benefited from the higher blanket temperatures to increase their efficiency by approximately 5 %. Lastly, the SCLL benefited the most from the higher blanket temperatures (1050 °C) by increasing its efficiency

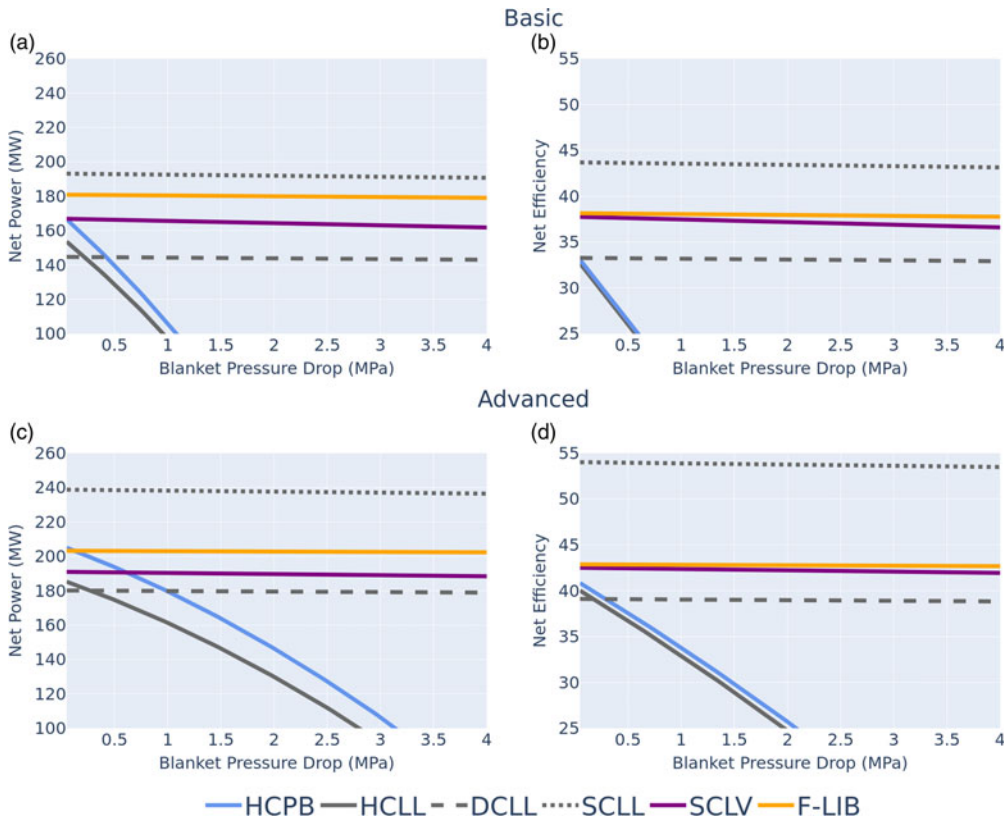


FIGURE 7. (a) Net power with respect to pressure drop for basic concepts, (b) net efficiency with respect to pressure drop for basic concepts, (c) net power with respect to pressure drop for advanced concepts and (d) net efficiency with respect to pressure drop for advanced concepts.

to approximately 50%. Under these conditions, all of these blanket concepts easily achieve the initial objective of producing 100 MW_e . In the case that an intermediate loop is not included for the baseline HCPB and HCLL, both the net power and the efficiency increase by approximately 10% as in the base cases.

4.4. Infinity Two point design

If the fusion power needs to be increased, the thermal performance of the blanket concepts and associated Rankine cycle remains practically unchanged assuming the same temperatures, temperature differences and pressures are used. Although the overall pumping power increases due to a higher mass flow rate requirement, this is balanced by a higher turbine output. These factors offset each other, resulting in similar net efficiency, while net power increases with higher fusion power. Table 6 presents the results of the Rankine cycle analysis for the Infinity Two point design with a fusion plasma power of 800 MW_{th} using an HCPB with reheat and no intermediate loop. A four corners approach employed by the ARIES system study program (Kessel *et al.* 2015) was used to explore the potential range of power outputs and efficiencies for the thermal cycle. In this analysis, the base case assumed

Parameter		Design improvement	Pressure drop improvement	Combined
Materials	Baseline	Advanced	Baseline	Advanced
Blanket pressure drop ¹	5 %	5 %	2.5 %	2.5 %
Efficiency (%)	32.58	37.78	35.74	39.95
Net power (MW)	323	375	355	399

¹Percent of thermal power using baseline parameters.

TABLE 6. Rankine cycle four corner analysis.

that recirculating power requirements are primarily driven by the thermal system, with a total pumping power requirement of 49.61 MW (5 % of the thermal power). The steady-state plasma heating and recirculating power for other systems such as the cryogenic and TFC plants were assumed to be negligible. From this, it can be concluded that a net efficiency of at least 30 % is readily achievable using a Rankine cycle and reasonable margins exist for accommodating uncertainties moving forward into the design. In addition, opportunities for improvement also exist, including improvements in blanket/primary loop design to reduce pumping power requirements, utilization of advanced materials for larger temperature windows and ultimate upper end temperature limits, and detailed design of the Rankine cycle to employ reheaters/preheaters and advantageous allocation of the steam flow rates. In addition, Brayton cycles will also be explored as *FusionDirect* develops to assess opportunities for continued improvements in thermal efficiency (Syblik *et al.* 2019). Key uncertainties include pressure drops based on higher fidelity engineering designs, as well as recirculating power requirements for the other support systems in the plant. These will be the subject of future work.

5. Tritium fuel cycle analysis

5.1. Introduction

Following the work of Abdou *et al.* (2021) and Meschini *et al.* (2023), a series of dynamic system-level models based on the RTM were developed for the TFC and applied to a relevant space of interest to understand the implications of various system and technology choices. In the RTM, the TFC is represented by a high-level model with constant flow rates in and out of each component, which can be described by zero-dimensional time-dependent ordinary differential equations. For the sake of simplicity, flexibility, speed and computational resource requirements, no detailed physics modeling of each component was performed. Some of the key system-level parameters examined in this study include fusion plasma power (P_f), plant availability factor (AF), tritium burn efficiency (TBE), direct internal recycling fraction (DIR), reserve time (t_r), doubling time (t_d), breeding zone (BZ) resident time (τ_{BZ}), tritium extraction system (TES) efficiency (η_{TES}), coolant purification system (CPS) efficiency (η_{CPS}), tritium start-up inventory (I_0), operational inventory ($I_{\text{operational}}$) and required tritium breeding ratio (TBR_{req}). It is important to note that TBR_{req} is not the same as the TBR referenced in § 3, but is instead the minimum

TBR target which is required to meet a prescribed doubling time for a specific TFC architecture. For additional discussion of the RTM model, including a description of specific subsystems, components, technology options, mathematical formulation and system-level parameters, readers are referred to Abdou *et al.* (2021) and Meschini *et al.* (2023).

In addition to the system-level parameters above which have been examined in previous studies, several new blanket specific parameters were identified and examined as potential drivers of the overall TFC dynamics.

- (i) Tritium loss fraction in the blanket (ϵ_{BZ}) assuming that tritium may permeate into and become sequestered in structural or functional materials in vessel, which has been identified as a potential issue both from a feasibility and safety perspective (Zinkle *et al.* 2013).
- (ii) Tritium flow fraction from the heat exchanger to the detritiation system ($f_{\text{HX} \rightarrow \text{detritiation}}$), which describes the fraction of tritium that permeates through the blanket side of the heat exchanger wall into a sweep gas, assuming a heat exchanger with an active tritium removal system, which is then fed to the water detritiation system.
- (iii) Tritium direct blanket processing fraction (DBP) for blanket tritium removal. The DBP has been explored in various fuel cycle designs (Meschini *et al.* 2023) but never systematically investigated. Similar to DIR, the purpose of DBP is to carry a fraction of the bred fuel directly from the TES to the storage and management system, thus bypassing the isotope separation system and shortening processing times.
- (iv) TES bypass fraction ($f_{\text{BZ} \rightarrow \text{HX}}$), which describes a design parameter whereby a fraction of tritium containing breeding medium/coolant bypasses the TES and is instead diverted directly to the heat exchanger. This may be advantageous for dual or self-cooled systems for thermal conversion efficiency reasons.

5.2. Parametric TFC analysis

The purpose of this initial application of the RTM was to understand at a high level the implication of different design choices on the TFC of high-field stellarator configurations. The three different TFCs used in this portion of the analysis are shown in Appendix A, figure 16, building on prior work (Abdou *et al.* 2021; Meschini *et al.* 2023). Only the components that have been modeled are shown in the figure and the inner fuel cycle (IFC) remained unchanged between blanket systems. The IFC layout used in this analysis was the same as Abdou *et al.* (2021), which utilized a more conservative definition of DIR. For the outer fuel cycle (OFC), three general layouts were developed consistent with the various types of fluid flows from the blanket, which is dictated by the usage of both separate cooling and self-cooling.

The analysis itself used a simple but effective approach known as the one-at-a-time sensitivity analysis (Hamby 1994), which has been used to great effect for analyzing TFC sensitivities for a EUROfusion DEMO-like device (Abdou *et al.* 2021), Commonwealth Fusion System's Affordable, Robust, Compact (ARC)-class device and the UKAEA's Spherical Tokamak for Energy Production device (Meschini *et al.* 2023). Table 7 lists the parameters and the range of values considered in this study, with table 8 listing the blanket design specific values, as well as resulting inventories and TBR_{req} for each of the seven blanket designs base cases.

Parameter	Symbol	Value	Range	Units	Steps
Fusion power	P_f	1000	400-1800	MW _{th}	5
Availability factor	AF	0.8	0.25–0.95	–	5
Tritium burn efficiency	TBE	0.01	0.005–0.05	–	5
Direct internal recycling fraction	DIR	0.25	0–1	–	5
Reserve time	t_r	24	0–48	H	5
Doubling time	t_d	5	1–10	Y	5
Breeding zone residence time	τ_{BZ}	1	0.1–240	H	9
TES efficiency	η_{TES}	1	0.2–0.9	–	9
CPS efficiency	η_{CPS}	0.95	0.25–0.95	–	5
Blanket loss fraction	ϵ_{BZ}	0	0–10 ^{–2}	–	5
Tritium flow fraction from the heat exchanger to the detritiation system	$f_{BZ \rightarrow \text{detritiation}}$	10 ^{–4}	0–10 ^{–2}	–	5
Direct blanket processing fraction	DBP	0	0–1	–	5
TES bypass fraction	$f_{BZ \rightarrow HX}$	0	0–0.95	–	5

¹These values vary by blanket concept as shown in [table 8](#).

TABLE 7. Fuel cycle parameters employed for the parametric analysis.

Parameter	Symbol	HCPB	HCLL	DCLL	Slow DCLL	Fast SCLL	F-LIB	SCLV	Mean	SD
Breeding zone residence time	τ_{BZ}	24	2.4	2.4	0.1	0.1	1.25	1.25	4.5	8.01
TES efficiency	η_{TES}	0.95	0.9	0.9	0.8	0.8	0.7	0.2	0.75	0.24
TFC schematic (figure 16)	-	a	a	b	b	c	c	c	-	-
Start-up inventory	I_0	7.06	6.92	6.92	6.92	6.92	6.96	7.47	7.02	0.19
Operational inventory	$I_{\text{operational}}$	3.29	3.14	3.14	3.14	3.14	3.18	3.84	3.27	0.24
Required tritium breeding ratio	TBR_{req}	1.09	1.09	1.09	1.09	1.09	1.09	1.10	1.09	0.00

TABLE 8. Blanket specific parameters, base case inventories, and TBR_{req} for the seven blanket concepts evaluated in the parametric analysis.

From [table 8](#), it can be inferred that the choice of blanket is not a strong driver of either inventory or breeding requirements given the chosen system-level parameters. The only discernible difference is driven by the modest increase in operational inventory of the OFC for the HCPB and SCLV. In order to better quantify sensitivities beyond a single data point for each concept, the approach of determining

relative sensitivity utilized by Meschini *et al.* (2023) was employed. In this approach, a relative sensitivity index coefficient (RIC) is calculated for each parameter in order to identify the relative importance of each. The mean RIC for each of the thirteen parameters is shown in figure 8(a), with radar plots showing the deviation of each blanket concept with respect to the mean in figure 8(b–d).

As can be seen, the main drivers of I_0 are TBE, P_f , t_r and DIR; $I_{\text{operational}}$ shares three of the same drivers (TBE, P_f and DIR) but is largely independent of t_r . In its place, it is more dependent on τ_{BZ} and η_{TES} , which dictates operational inventory in the blanket; TBR_{req} is independently driven by AF and t_d which impacts breeding requirements directly; TBR_{req} is also driven indirectly by TBE, t_r and DIR through their impact on I_0 , which requires a corresponding shift in TBR_{req} to maintain a prescribed t_d ; TBR_{req} is largely independent of P_f , even though both I_0 and $I_{\text{operational}}$ have a relatively high dependency on this parameter. This is due to the net increase in neutron production with increasing P_f , thus keeping TBR_{req} largely unchanged. Given the relatively low TBE and DIR of the assumed reference case, the inventory in the IFC dominates the overall system and the parameters which dictate that inventory (TBE, P_f , t_r and DIR) dominate the overall dynamics of the system. The implications of this can be seen with DBP which has essentially no relevancy on the overall system dynamics, whereas the analogous DIR is a key parameter. For this analysis there were no parameters for which the RIC had both a significant value and difference in sign between I_0 , $I_{\text{operational}}$ or TBR_{req} . This implies that an overall system can be designed which optimizes (i.e. minimizes) all three parameters simultaneously without the need for significant tradeoffs.

Figure 8(b–d) illustrates the difference in performance for the various blanket concepts. As is shown, the HCLL, SCLL, F-LIB and both slow and fast flowing DCLL concepts all behave relatively similarly. This is due to a net combination of both relatively low τ_{BZ} and adequately high η_{TES} , which minimizes the overall blanket inventory. The HCPB and SCLV are the outlier systems due to their relatively high τ_{BZ} (24 h for the HCPB) and low η_{TES} (0.2 for the SCLV). The HCPB is relatively sensitive to changes in η_{TES} , where sizable decreases can result in relatively large tritium inventories being fed back to the BZ, which has the longest τ_{BZ} of all the reference systems. The SCLV is more sensitive to changes in τ_{BZ} , where sizable increases can result in large tritium inventories due to the inadequate removal of tritium from the breeder medium, which is the lowest of all the concepts. The SCLV is also more sensitive to both $f_{\text{BZ} \rightarrow \text{HX}}$ and ϵ_{BZ} due to the larger tritium inventory in the blanket for these concepts. Interestingly, the SCLV is less sensitive in a relative sense to TBE than the other systems even though it experiences the same general relationship trends. This is due to the fact that the SCLV has the highest blanket operational inventory of the reference systems, which places more of the overall ‘sensitivity budget’ in the other parameters discussed previously.

These plots represent a small subset of the data obtained from the parametric study at large and are shown to illustrate the quantitative approach to the TFC analysis in this study. In general, these findings are consistent with prior studies, and seem to imply that for the reference parameters selected (i.e. relatively low TBE and DIR) the different blanket concepts perform quantitatively similar to one another within margins so long as adequately low τ_{BZ} (less than approximately 24 h) and high η_{TES} (greater than 0.6) are maintained.

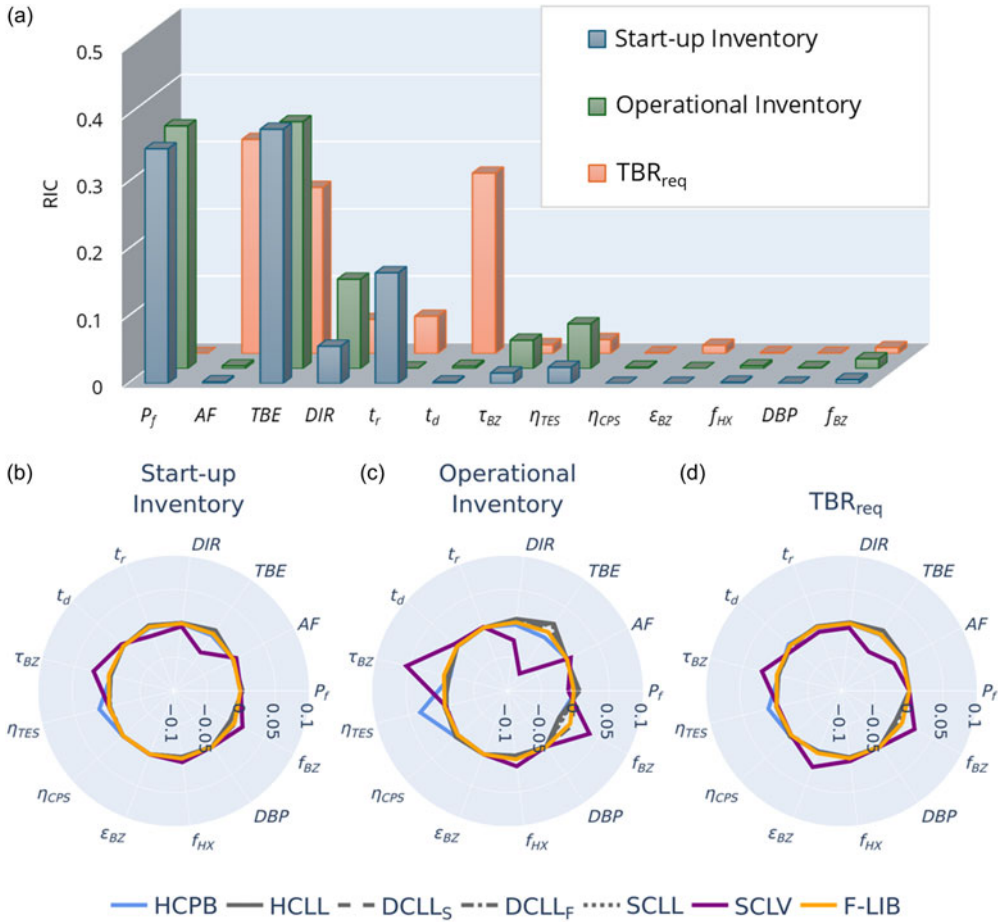


FIGURE 8. (a) Mean RIC and radar plots of (b) RIC deviation for the I_0 , (c) $I_{operational}$ and (d) TBR_{req} .

5.3. TFC scenario development

Building upon this parametric study, the next step was to delve deeper into specific TFC architectures to better understand scenarios for Infinity Two and attempt to understand viable R&D pathways for reducing overall tritium inventories and breeding requirements. This included the development of a more bespoke TFC model as well as examination of various operating points for Infinity Two. From the TFC model perspective, cross-referencing more contemporary literature such as the EU DEMO fuel cycle preconceptual design activities (Day *et al.* 2022), it becomes apparent that the architectures proposed by Abdou *et al.* (2021) and Meschini *et al.* (2023) can be improved upon. As examples, the prior formulations did not explicitly capture the dynamics of both the DIR and fueling system, so those inventories are lost from consideration even though they are expected to be non-trivial given the required fueling throughput of the plasma (Schwenzer *et al.* 2022). In addition, the models assumed that tritium not sent to the DIR system is instead sent to the isotope separation system for full separation, which is both non-ideal and unnecessary for a steady-state MFE system where the IFC DT mixture simply needs to be rebalanced

Parameters	Baseline	Technology advancement	Physics advancement	Both advancements
AF	80 %	95 %	80 %	95 %
DIR	80 %	95 %	80 %	95 %
η_{TERS}	80 %	95 %	80 %	95 %
τ_{BZ}	24 h	1 h	24 h	1 h
TBE	1 %	1 %	5 %	5 %
I_0^1	3.701 (0.655) kg	3.423 (0.372) kg	1.017 (0.408) kg	0.843 (0.233) kg
$I_{\text{operational}}^1$	0.673 (0.667) kg	0.382 (0.379) kg	0.417 (0.416) kg	0.238 (0.237) kg
$\text{TBR}_{\text{req}}^1$	1.040 (1.022)	1.031 (1.016)	1.012 (1.008)	1.008 (1.005)

¹The first value in each cell is the nominal parameter value obtained with $t_r = 24$ h. The second value in each cell is the tritium-lean parameter obtained with $t_r = 0$.

TABLE 9. TFC four-corners analysis.

and kept below a certain protium content (typically of the order of 1 %) prior to reinjection.

In order to provide a more realistic estimate of TFC parameters in Infinity Two, a new three-loop fuel cycle model shown in [Appendix A, figure 18](#) was generated consistent with the proposed architecture of Day *et al.* (2022) from the EU DEMO pre-conceptual design which utilized the HCPB blanket concept. This model focuses on: (i) maximizing DIR fraction with an aggressive 80 % baseline, (ii) the addition of an intermediate loop with an isotope rebalancing and protium removal system and (iii) accurate accounting for all component inventories. The main driver for these changes is the desire to avoid isotopically separating large amounts of tritium, which for existing technologies such as cryogenic distillation, can lead to large inventory issues associated with the liquid hold-ups, negatively affecting safety and operating costs. For a more detailed explanation of this general architecture, including a rigorous technological assessment and technology choices for each component, readers are directed to Day *et al.* (2022). Not all of the relevant parameters for the model are presented in the literature, including residence time and flow fractions for the various components and subsystems, so a new RTM model had to be constructed from the ground up. The initial model was created using a combination of assumptions from the prior RTM models and flow fractions derived from flow rates and partial pressures presented in Day *et al.* (2022). Once an initial model was established, the residence time in the various components was quantified using the steady-state tritium inventories computed by Schwenzer *et al.* (2022) and the approach of Meschini *et al.* (2023). For this approach, TFC simulations were run in a systematic fashion using the EU DEMO parameters with an HCPB blanket ($P_f = 2$ GW, $\tau_{\text{BZ}} = 24$ h, $\eta_{\text{TES}} = 0.8$, TBE = 0.6 %) and the component residence times were varied one at a time until the relevant component tritium inventories converged to within half a gram of the values listed in Schwenzer *et al.* (2022).

Once the parameters were set, this model was scaled to the Infinity Two configuration with $P_f = 800$ MW and used to model a number of commercial power plant scenarios. The baseline scenario assumed conservative technology values based on

the HCPB EU DEMO ($\text{DIR} = 0.8$, $\tau_{\text{BZ}} = 24$ h, $\eta_{\text{TES}} = 0.8$) but with a commercially relevant $\text{AF} = 80\%$. A relatively conservative physics assumption of $\text{TBE} = 1\%$ was also used in this baseline, and a standard value of $t_d = 5$ years was used across all scenarios. A four corners approach employed by the ARIES system study program in Kessel *et al.* (2015) and Meschini *et al.* (2023) was then used to examine a variety of advanced and conservative scenarios to better illustrate how the relevant TFC parameters can vary with different R&D emphasis moving forward. The results of this analysis can be seen in table 9. Here, technology advancement assumes $\text{DIR} = 0.95$, $\tau_{\text{BZ}} = 1$ h, $\eta_{\text{TES}} = 0.95$ and $\text{AF} = 95\%$, and the physics advancement assumes $\text{TBE} = 5\%$. The initial value in each box represents the TFC parameters using a standard assumption of reserve inventory ($t_r = 24$ h with a failure fraction of 25%), and the second value represents these parameters under a tritium-lean scenario where there is no reserve inventory.

As can be seen from this table, using modern architecture and technology/physics assumptions, the operational tritium inventory of a $P_f = 800$ MW power plant can be driven well below one kilogram (675 g as a baseline), and even go as low as half or quarter of a kilogram (238 g in the most optimistic scenario) with additional improvements in both processing and plasma performance. The start-up inventory in this parameter space is primarily driven by reserve inventory requirements, which scale with P_f and as the inverse of TBE. This reserve inventory requirement can push start-up inventory values to a factor of 5–10 higher than would otherwise be necessary from a purely operational standpoint. A key finding of this analysis shows that the requirement for a significant reserve inventory should be revisited for power plants operating in this physics and technology space, to avoid significant and likely unnecessary inventories of tritium being sequestered away in storage to decay. This will likely require a focus on other approaches to ensuring a robust TFC. Finally, it should be noted that TBR_{req} for such a facility is relatively low (less than 1.05), even for a 5-year doubling time, giving confidence that tritium self-sufficiency is in fact achievable from a breeding perspective and that the roll out of a large fusion ecosystem may not be as constrained as previously postulated (Abdou *et al.* 2021).

Finally, a number of scenarios specific to the Infinity Two start-up phase were evaluated. In these scenarios, it was assumed that a phased approach to DT operation will be employed such that the plasma-on time progressively increases towards a commercially relevant duration of 18–24 months with an AF of at least 80%. This staged approach helps to improve operational confidence and progressively bootstraps plasma and neutron fluence levels up to commercially relevant levels for critical components, thus allowing for simultaneous development during the operation of the facility (Kessel *et al.* 2018). For this analysis, a number of scenarios were run using the baseline technology and physics assumptions of the four corners analysis and AF spanning 33% to 80%. The plasma-on times of the various phases were set such that there were six months of downtime between operation to allow for inspection and maintenance. It was also assumed that no reserve inventory would be held given both the relatively large inventory requirements discussed previously but also the anticipated lack of knowledge on both mean time between failures and mean time to recovery of the system. Finally, instead of a set doubling time, breeding requirements were derived such that the inventory maintained an adequate level during the plasma off-time and the facility could restart operations again without the need to purchase additional tritium. The results of this analysis indicate that even in the case of low availability (33%), the TBR_{req} is very modest (approximately 1.023) for the Infinity Two start-up phase. This is also consistent with what is expected in

that of a higher availability commercial system, assuming an overall similar TFC architecture and design space is used.

6. Discussion

In addition to the high-level quantitative analyses described in §§ 3, 4 and 5, a qualitative evaluation was performed to gauge the potential of each of the reference concepts against the **FusionDirect** objectives in categories which could not be quantitatively evaluated under the given timescales and resources. This qualitative analysis reviews and builds upon the significant body of work focused on comprehensive blanket evaluations including the Blanket Comparison and Selection Study (Smith *et al.* 1985), various ARIES activities (El-Guebaly *et al.* 2005; Kessel *et al.* 2015), the EU DEMO Blanket Program (Hernández *et al.* 2023; Federici *et al.* 2014; Stork *et al.* 2014) and other miscellaneous surveys (Raffray *et al.* 2002; Meier 2014). The primary and most important finding of this qualitative evaluation is that in isolation an overall top-rated blanket concept is not readily apparent at such an early stage of development. In general, each concept has both advantages and disadvantages when compared directly against alternatives, and the outcome of any evaluation is highly dependent on assumptions and design objectives for the device in question. In addition, each blanket concept must be paired with a specific confinement concept to determine suitability for an integrated, economically viable energy producing system. In this regard, there are relatively few stellarator design studies to date, many of which were not wholly self-consistent (Najmabadi *et al.* 2008; Warmer *et al.* 2016). This emphasizes the need for more thorough and comprehensive design activities moving forward.

A second and broadly applicable finding is that the selection and development of appropriate materials, particularly structural materials, is a driving consideration for both the performance and deployability of all fusion blanket concepts. Numerous factors must be considered in the selection of appropriate materials, including material availability and cost, fabricability, joining techniques, mechanical and thermophysical properties, radiation effects, chemical compatibility and corrosion issues, safety and waste disposal aspects and nuclear properties. For designers, a particularly important consideration when selecting materials is the expected operating conditions, including mechanical, thermal and radiation loading environments during the lifetime of the component. It should be stressed that the detailed minimum and maximum operating temperature limits for a given structural material are strongly dependent on the specific system design and manner in which these materials will be employed (Zinkle & Ghoniem 2000; Zinkle & Snead 2014), but will also dictate overall thermal performance as shown in § 4. In this regard, a blanket concept cannot be truly understood without also having a rigorous understanding of materials performance in the prescribed environment, including degradation of that performance over its operating life. A recent effort by the US fusion materials community and the Electric Power Research Institute attempted to capture these materials considerations, including a technology readiness assessment and technology road map for leading material systems, and readers are directed there for further details (U.S. Fusion Materials Coordinating Committee 2024).

Finally, it should be noted that while Infinity Two needs to demonstrate commercial relevance, it is not itself a commercial system. Given the relative maturity of blanket technology and the aggressive developmental timelines, it is unlikely that a concept will be deployed under the **FusionDirect** program which is fully optimized

prior to a first-of-a-kind commercial plant. In this regard, emphasis is placed on identifying a baseline blanket which can be rapidly deployed for Infinity Two while also maintaining flexibility and opportunities for higher performing concepts later in development. What follows is a discussion of key findings for the six blanket concepts considered in this study, a graphical summary of which can be found in [figure 9](#).

6.1. Solid breeders: the promising solution

Solid breeders, specifically ceramic-based solid concepts, are currently considered to be the baseline approach internationally. The primary motivation for the development of solid breeder blankets stems from the desire to overcome the limitations of liquid breeders, including a focus on higher chemical inertness, elimination of MHD effects and mitigation of corrosion concerns (Johnson *et al.* 1988). In addition, solid breeders also tend to have higher lithium densities than liquids, which, in combination with inherent moderating elements such as oxygen, make them advantageous for designing more compact blankets from both a breeding and shielding perspective. For these reasons, solid blankets have been seen as a favored approach since the 1980s, with extensive international R&D programs aimed at confirming the suitability of solid breeders designs from both a materials science and engineering perspective (van der Laan *et al.* 2000). They are also the most heavily invested-in blanket concept from the international public programs. To illustrate this point, it should be noted that four of the six Test Blanket Modules planned as part of the ITER program will utilize solid blanket designs (Giancarli *et al.* 2020). Recent preconceptual design studies in support of the EU DEMO program have shown that existing solid breeders are high-performing and robust blanket candidates while also enjoying a relatively mature technology basis, thanks in large part to their usage of leading RAFM steels as the structural material (Zhou *et al.* 2023a). They also have strong and reliable performance when compared against the other concepts, as verified in all three analyses presented previously as well as preconceptual design studies under the EU DEMO program (Zhou *et al.* 2023a). In particular, the neutronics performance appears to pair well with T1E stellarator designs. Finally, their performance in off-normal events is also anticipated to be more predictable due to the solid fuel form and usage of inert He coolant, which is seen as advantageous for early fusion nuclear systems (Jin & Yin 2017).

Although a significant R&D effort on ceramic breeder development has laid a strong foundation over the past several decades, there are still challenges which must be addressed. First is the traditional reliance on beryllium multipliers in order to achieve adequate TBR, which represents a potential safety, supply chain and cost issue (Scaffidi-Argentina *et al.* 2000; Longhurst *et al.* 2011; Kolbasov *et al.* 2016; Shimwell *et al.* 2016). The second challenge is related to the thermal and mechanical behavior of solid breeder materials under the complex nuclear fusion loading conditions, particularly at long time scales, which can lead to significantly degraded materials properties, induce volumetric change, lead to breeder performance drops and potentially affect chemical behavior leading to increased interaction with structures and/or induce lithium transport within the blanket (van der Laan *et al.* 2016). Combined with the need for existing designs to shut down in order to refuel, this can have implications on the overall commercial system viability. The third challenge relates to tritium extraction from the ceramic materials in vessel, which comprises

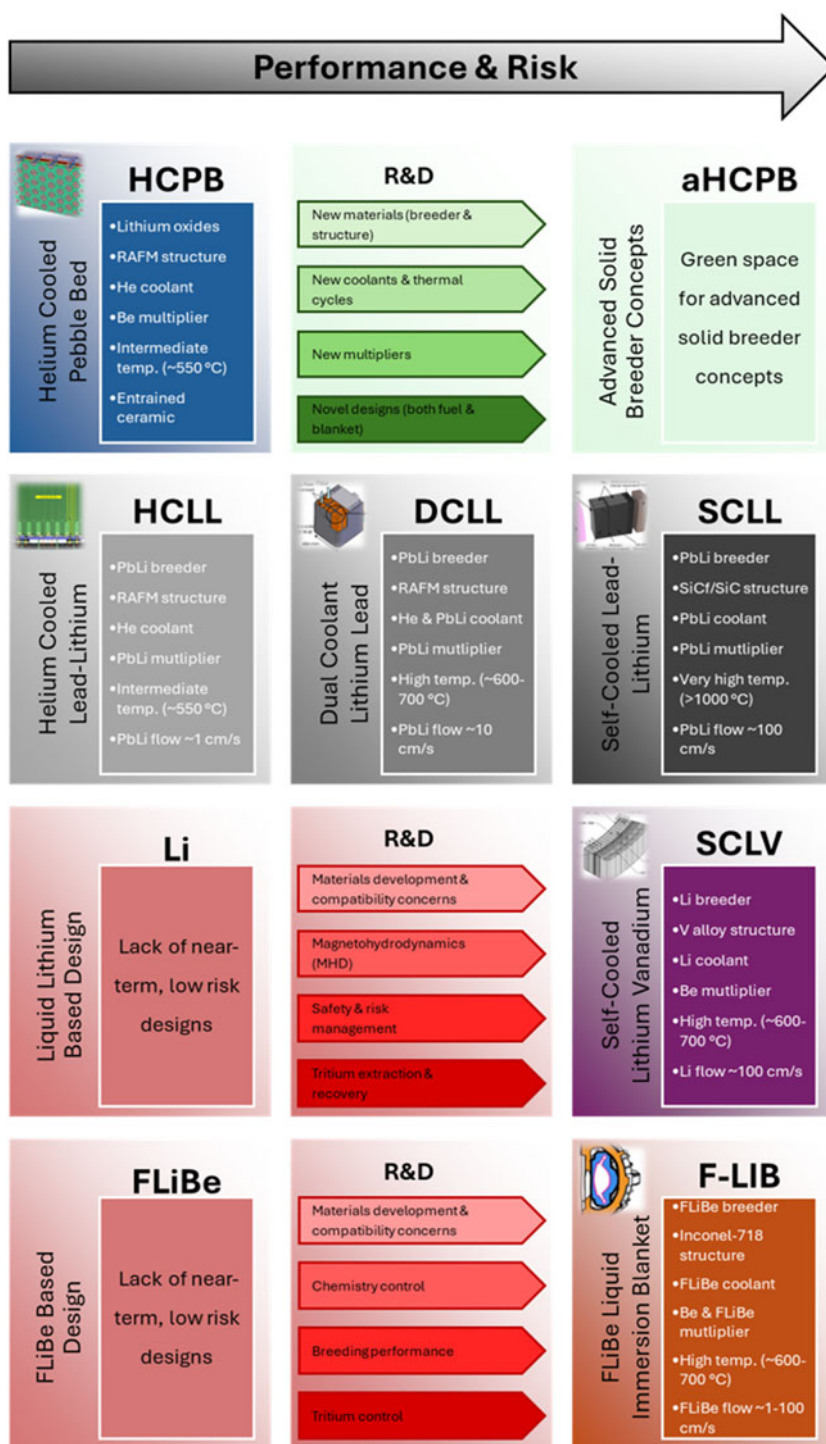


FIGURE 9. High-level comparison of the status and developmental pathways for various fusion blanket concepts. Green arrows indicate R&D opportunities for advancing performance of proposed concepts while red arrows indicated required R&D prior to the implementation of proposed concepts.

complex, multi-physics interactions due to a variety of factors including steep temperature gradients, radiation-induced defects that can act as traps and complex chemistry of the system due to lithium burn-up and/or residual impurities in the sweep gas. Understanding and appropriately accounting for this tritium release is critical both from a safety and fuel cycle viability perspective (van der Laan *et al.* 2016; Cristescu & Draghia 2020; Simon *et al.* 2022). Lastly, the relatively large volume of ceramic breeder and multiplier required for breeding blankets in future power systems and the need for regular refueling in order to maintain breeding performance will necessitate safe and economical solutions for reprocessing and recycling, thus minimizing cost and waste (Leys *et al.* 2021). However, several R&D avenues have been identified to address these shortcomings, including using new materials (Zinkle *et al.* 2017; Hernández & Pereslavytsev 2018; Davies & Murphy 2021; Samolyuk & Edmondson 2021; Bhattacharya *et al.* 2022; Bhardwaj *et al.* 2024), coolants (Syblik *et al.* 2019; Wang *et al.* 2019; Wu *et al.* 2020), multipliers (Hernández & Pereslavytsev 2018; Zhou *et al.* 2019; Gaisin *et al.* 2020) and designs/design methodology (Shimwell *et al.* 2016; Sharafat *et al.* 2016; Badalassi 2024) to better meet the needs of stellarators.

6.2. PbLi-based breeders: a compelling alternative

PbLi-based designs are the second most mature family of concepts, with the slow flowing concepts having near equal footing with solid breeders in terms of technical maturity, due in large part to the reduced MHD related issues compared with fast flowing concepts (Hernández *et al.* 2023). In addition, these designs mitigate most, if not all, of the primary risks associated with ceramic breeders, including reliance on Be, mitigation of radiation and thermal stability issues, online tritium extraction/refueling and potential dual usage as a coolant for design simplification. As shown in the analysis above, PbLi designs have performance which could be an appropriate if not optimal match for T1E blanket requirements should the issues with solid breeders prove insurmountable. In addition, PbLi-based concepts have a well-established developmental pathway which is relevant for both near-term systems such as Infinity Two as well as longer-term, higher-performance commercial systems. This is due to the staged implementation pathway for the HCLL to DCLL to SCLL, which can be implemented over time as higher performing materials become available and operational basis improves (Smolentsev *et al.* 2015; Tillack *et al.* 2022). Currently the PbLi-based family of blankets is the only one which has such a well-defined developmental pathway. In addition, the HCLL and DCLL designs share many similar R&D pathways with the solid blanket concepts as they are all currently proposing Fe-based materials as the primary structure, which is beneficial from a leveraging and risk mitigation standpoint. For these reasons, the DCLL has been the favored design in the US fusion program over the past several decades (Abdou *et al.* 2015; Kessel *et al.* 2018) and is seen as a potential risk-mitigating fallback design for *FusionDirect*.

However, PbLi also has its own share of challenges. Similar to pure lithium, PbLi suffers from being chemically reactive with water and air, although to a lesser extent (Malang & Mattas 1995), it has potentially severe compatibility issues with structural materials (Romedenne *et al.* 2023) and finally tritium extraction is not a fully solved problem, although there is a stronger technology basis than for pure lithium (Garcinuño *et al.* 2018; Humrickhouse & Merrill 2018). An additional issue specific

to the DCLL and SCLL concepts which propose to utilize the PbLi as a coolant is that of MHD effects which result from a conducting material being flown in a high background magnetic field environment. This can increase pumping power requirement (due to MHD pressure drop), inhibit heat transfer (via suppression of turbulent flow) and complicate tritium and corrosion product transport (Smolentsev 2021) and in general is not a well-understood phenomenon at fusion relevant conditions. Next, as a breeder the performance of PbLi is not as high as that of either the solids breeders or pure lithium, and PbLi concepts typically require ^6Li enrichment greater than 90 wt% in order to achieve similar breeding levels, as shown in the neutronics analysis and the literature (van der Laan *et al.* 2016). Finally, lead-lithium alloys have some specific design challenges such as the high density resulting in the requirement for stronger structures to limit mechanical stresses and potential challenges associated with liquid metal spills which could be challenging to clean (Hernández & Pereslavytsev 2018; Piet *et al.* 1987).

6.3. Pure lithium and FLiBe-based breeders: not the right fit

Both pure lithium and FLiBe-based concepts, while novel and potentially promising, are seen as being the least mature concepts as well as somewhat niche in application space. While they offer similar benefits as the PbLi concepts (no radiation/thermomechanical damage in the breeder material, online tritium extraction/refueling and potential dual usage as a coolant), they both require dedicated developmental pathways which are tangential from solid and PbLi blanket concepts. This is due in large part to requirements for new structural materials, unique technologies associated with tritium extraction and chemistry control, and the general incompatibility with separately cooled or dual-cooled approaches (though this is being revisited in the case of lithium (Lord *et al.* 2024)). In this respect they lack readily apparent, nearer-term implementable designs and so present an ‘all or nothing’ investment paradigm that makes them high risk for a venture such as **FusionDirect**.

It is also important to note that proponents pursuing these concepts are motivated at least in part by confinement concept considerations which differ from that of the T1E high-field stellarator approach. For pure lithium, development is largely being driven by confinement concepts where the in-vessel volume is bifurcated into segments of shield-only builds (due to space constraints) and largely unconstrained builds which must optimize breeding (in order to accommodate the loss of breeding volume in those shield-only volumes). Such is the case for spherical tokamaks where the compact nature and shape means the incorporation of a sizable inboard breeder blanket is not possible, and the outboard breeding must therefore be maximized in order to achieve tritium self-sufficiency (Lord *et al.* 2024). As can be seen from the parametric analysis in § 3, this is where lithium blanket concepts excel. The FLiBe-based designs are being driven by the desire to enable extremely compact devices, and so the associated blanket designs must maximize the shielding value of the breeding zone. As can be seen from the parametric analysis in § 3, this is where FLiBe concepts excel, although it does require design modifications elsewhere to ensure that the TBR requirements are met simultaneously. An example of this design trade-off space is the Commonwealth Fusion Systems’ ARC design (Sorbom *et al.* 2015), where structure and penetration in the breeding zone are kept to essentially zero in

order to achieve the required TBR (Segantin *et al.* 2020). This is not currently applicable to Infinity Two, where it is anticipated that the fueling systems, heating systems and coolant manifolds for the divertor and first wall will have non-trivial space claims in the blanket region, and maintenance approaches may require additional structure for modularization. Neither of the motivating factors for pure lithium or FLiBe are expected to apply to current or future T1E stellarator designs, but it is important to recognize these driving considerations and emphasize the need for performing blanket design early in the design life cycle to ensure the blanket concept integrates with the overall system requirements.

For lithium, additional technical challenges are primarily driven by the high chemical reactivity, which represents significant engineering and safety challenges. From an engineering perspective, the reactivity presents challenges for both structural and functional (i.e. insulators for mitigation of MHD effects) materials compatibility since lithium is reactive with many materials and alloying constituents proposed for fusion applications (Si *et al.* 2020; Muroga *et al.* 2009; Smith *et al.* 2000). Lithium will also suffer from MHD related issues similar to PbLi, but with higher electrical conductivity, and may prove difficult for the complex and strong magnetic fields of T1E stellarators (Smolentsev 2021). Related to both safety and engineering considerations is lithium's high affinity for tritium and the requirement that tritium concentration in the medium be kept low (approximately 1 appm) in order to maintain the blanket and overall plant tritium inventories to acceptable levels as shown in § 5. The low vapor pressure of tritium above molten lithium makes extraction of tritium difficult and requires the development of new extraction methodologies. Currently proposed extraction methods include the Maroni process (Maroni *et al.* 1975), direct electrolysis (Teprovich *et al.* 2019) and distillation columns (Christenson *et al.* 2018), all of which are relatively immature and need significant improvement to show power plant relevance. An additional safety consideration is that lithium is highly reactive to water, air and other substances, especially at the high temperatures expected in fusion energy systems. The resulting extreme exothermic reactions which could lead to confinement challenges for radiological inventories, such as mobilization of the tritium content in the lithium or release of activation products from the surrounding structures (Reyes *et al.* 2016).

The main challenge with utilizing FLiBe or other molten salts stems from a lack of compatibility with existing low activation structural materials. This is due to the relatively high melting point, particularly for FLiBe, which can narrow temperature design windows to unacceptably low levels when incorporating upper end structural material limits (Zinkle & Ghoniem 2000). Chemical compatibility with structural and functional materials is another concern, particularly under irradiation conditions which can lead to hydrofluoric acid production via radiolysis and requires tight chemistry control in order to avoid unacceptable corrosion (Pint *et al.* 2024). These are key concerns which may require the development of entirely new materials systems and could potentially hamper the deployment of molten salt blanket concepts in the near term. The final challenge is that of tritium solubility in FLiBe is extremely low and could result in elevated tritium loss via diffusion and trapping in blanket structural materials (Wong *et al.* 2005). Ultimately, these challenges, in combination with the difficulty of reaching an adequate TBR as outlined in § 3, make FLiBe or other salt-based blankets unattractive for *FusionDirect* at this point in time.

7. Conclusion

T1E is pursuing an ambitious and uniquely direct path to an FPP. This requires timely identification, analysis, evaluation and down selection of potential blanket concepts. The focus of this study was to identify a baseline blanket which can be rapidly deployed for the Infinity Two FPP while also maintaining flexibility and opportunities for higher performing concepts later in development. Guiding principles driving the study were identified, consistent with the overarching objectives of the *FusionDirect* program. A literature survey was conducted to establish reference concepts, of which six were identified: the HCPB, HCLL, DCLL, SCLL, SCLV and the F-LIB. Next, a series of quantitative and qualitative analyses were performed. This included a neutronics analysis for determining tritium breeding and shielding performance, a thermal analysis for determining overall system efficiency and net electric output potential, and a TFC analysis for understanding the impact of blanket choices and system parameters on closure of the fuel cycle. In conjunction with these quantitative activities, a qualitative study was performed to understand other design drivers which could not be captured via analysis.

The results of this comprehensive study indicated that the HCPB is the most promising concept for Infinity Two. This is primarily motivated by the neutronics performance at applicable blanket build depths, where the HCPB was able to achieve a TBR of 1.30 in low engineering fidelity simulations, as well as the relatively mature technology basis. In addition, there appears to be significant opportunity for continued improvement in this family of concepts using new materials, coolant, multipliers and designs. The PbLi family of concepts, particularly the DCLL, offers a compelling alternative to the HCPB. These concepts maintain similar developmental pathways while simultaneously mitigating much of the technical risk, namely reliance on Be, mitigation of radiation and thermal stability issues, online tritium extraction/refueling and potential dual usage as a coolant for design simplification. Both concepts are expected to enable reasonably high thermal efficiencies of greater than 30 % with a Rankine cycle. In addition, both concepts are compatible with a viable fuel cycle, with anticipated operational inventories of less than one kilogram (approximately 675 g) for an 800 MW_{th} fusion device and a required TBR (TBR_{req}) of less than 1.05.

Acknowledgements

The authors would like to acknowledge the support of the UW-Madison Center for High Throughput Computing (University of Wisconsin–Madison 2024b) for providing computational resources used to perform neutronics calculations.

Editor Per Helander thanks the referees for their advice in evaluating this article.

Funding

This work was supported by Type One Energy Group Inc.

Declaration of interests

The work of M.S.T. was performed as a consultant and was not part of the employee's responsibilities at the University of California-San Diego.

Appendix A. Additional figures

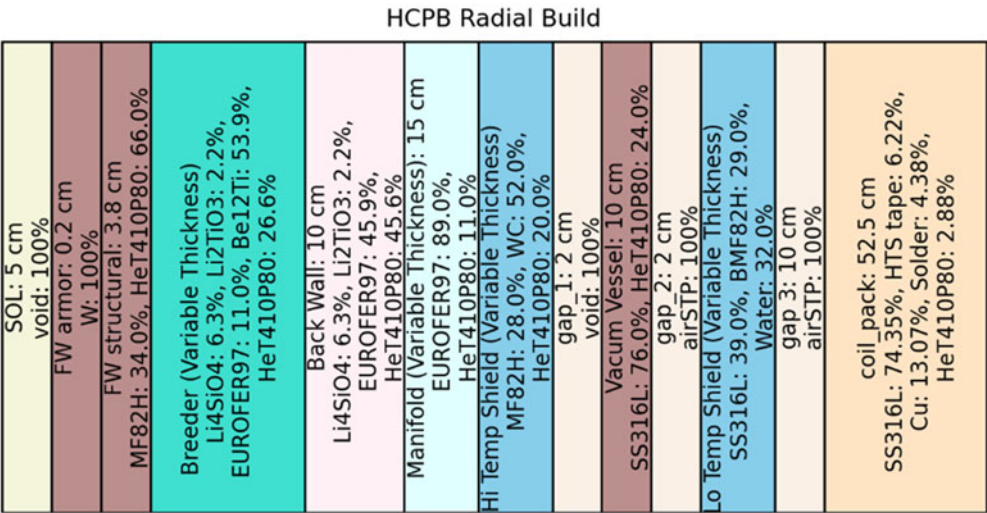


FIGURE 10. Radial build diagram of the concentric toroidal shell layers in the helium-cooled pebble bed blanket concept for this high-throughput parametric neutronic study. Material layers are based on those in (Zhou *et al.* 2023a, b); material compositions provided in volume percent.

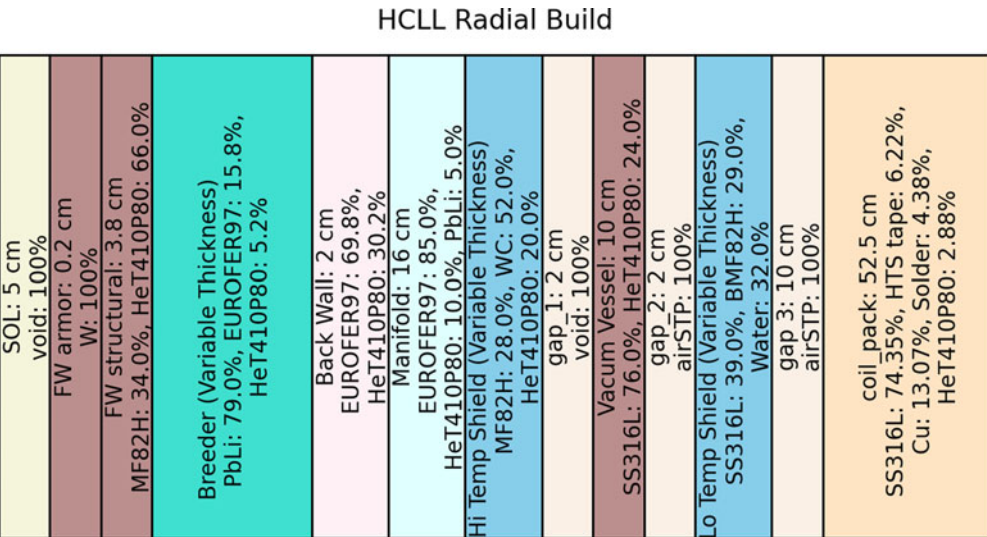


FIGURE 11. Radial build diagram of the concentric toroidal shell layers in the helium-cooled lead-lithium blanket concept for this high-throughput parametric neutronic study. Material layers are based on those in Aubert *et al.* (2018); Jaboulay *et al.* (2019); Aiello *et al.* (2014); material compositions provided in volume percent. The manifold layer was kept at a constant multiple of 0.2 times the breeder thickness.

DCLL Radial Build	
SOL: 5 cm void: 100%	
FW armor: 0.2 cm W: 100%	
FW structural: 3.8 cm MF82H: 34.0%, HeT410P80: 66.0%	
Breeder (Variable Thickness) PbLi: 77.0%, SiC: 3.5%, MF82H: 6.0%, HeT410P80: 13.5%	
Back Wall: 2 cm MF82H: 80.0%, HeT410P80: 20.0%	
Manifold: 6 cm MF82H: 30.0%, HeT410P80: 70.0%	
Hi Temp Shield (Variable Thickness): MF82H: 28.0%, WC: 52.0%, HeT410P80: 20.0%	
gap 1: 2 cm void: 100%	
Vacuum Vessel: 10 cm SS316L: 76.0%, HeT410P80: 24.0%	
gap 2: 2 cm airSTP: 100%	
Lo Temp Shield (Variable Thickness) SS316L: 39.0%, BMF82H: 29.0%, Water: 32.0%	
gap 3: 10 cm airSTP: 100%	
coil pack: 52.5 cm SS316L: 74.35%, HTS tape: 6.22%, Cu: 13.07%, Solder: 4.38%, HeT410P80: 2.88%	

FIGURE 12. Radial build diagram of the concentric toroidal shell layers in the dual-cooled lead-lithium blanket concept for this high-throughput parametric neutronic study. Material layers are based on those in Davis *et al.* (2018); material compositions provided in volume percent.

SCLL Radial Build	
SOL: 5 cm void: 100%	
Breeder (Variable Thickness) PbLi: 69.6%, SiC: 22.2%, void: 8.2%	
Hi Temp Shield (Variable Thickness) MF82H: 28.0%, WC: 52.0%, HeT410P80: 20.0%	
gap 1: 2 cm void: 100%	
Vacuum Vessel: 10 cm SS316L: 76.0%, HeT410P80: 24.0%	
gap 2: 2 cm airSTP: 100%	
Lo Temp Shield (Variable Thickness) SS316L: 39.0%, BMF82H: 29.0%, Water: 32.0%	
gap 3: 10 cm airSTP: 100%	
coil pack: 52.5 cm SS316L: 74.35%, HTS tape: 6.22%, Cu: 13.07%, Solder: 4.38%, HeT410P80: 2.88%	

FIGURE 13. Radial build diagram of the concentric toroidal shell layers in the self-cooled lead-lithium blanket concept for this high-throughput parametric neutronic study. Material layers are based on those in Kessel *et al.* (2015); material compositions provided in volume percent.

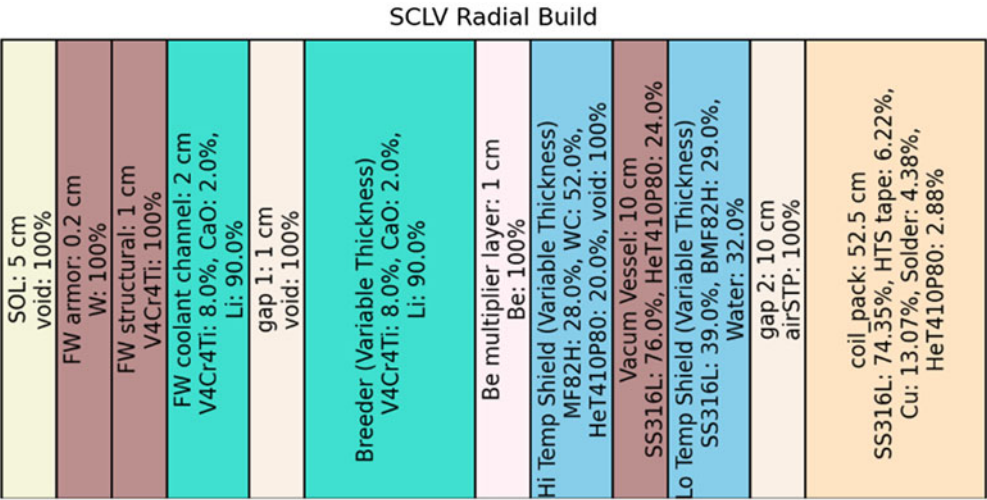


FIGURE 14. Radial build diagram of the concentric toroidal shell layers in the self-cooled lithium (breeder) vanadium (structure) blanket concept for this high-throughput parametric neutronic study. Material layers are based on those in Kessel *et al.* (2015); material compositions provided in volume percent.

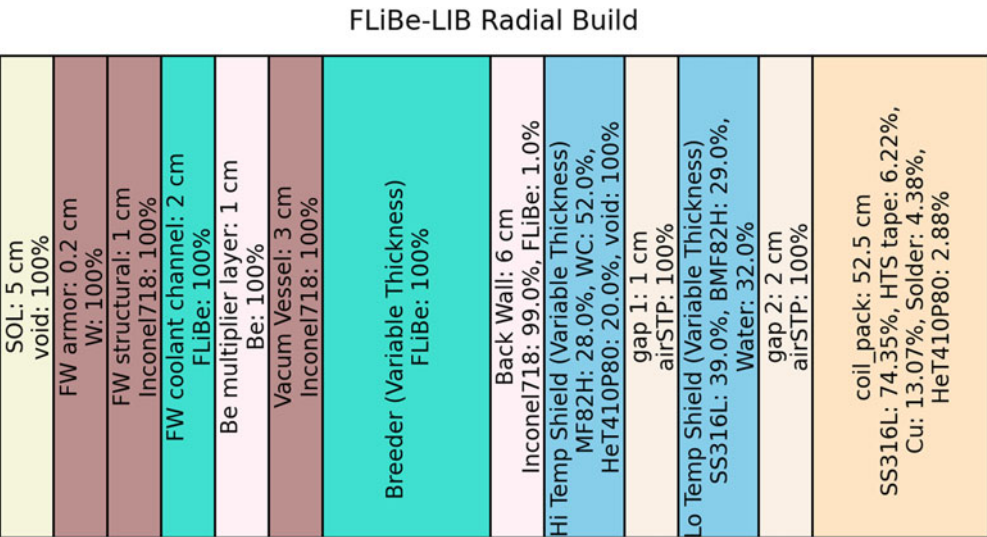


FIGURE 15. Radial build diagram of the concentric toroidal shell layers in the FLiBe liquid immersion blanket concept for this high-throughput parametric neutronic study. Material layers are based on those in Segantin *et al.* (2020, 2022); Bae *et al.* (2022); material compositions provided in volume percent.

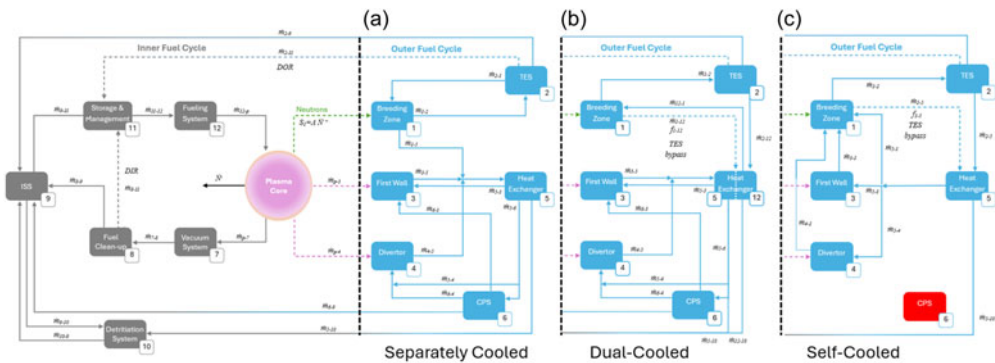


FIGURE 16. Parametric TFC layouts of (a) separately cooled blanket concepts, (b) dual-cooled concepts and (c) self-cooled concepts.

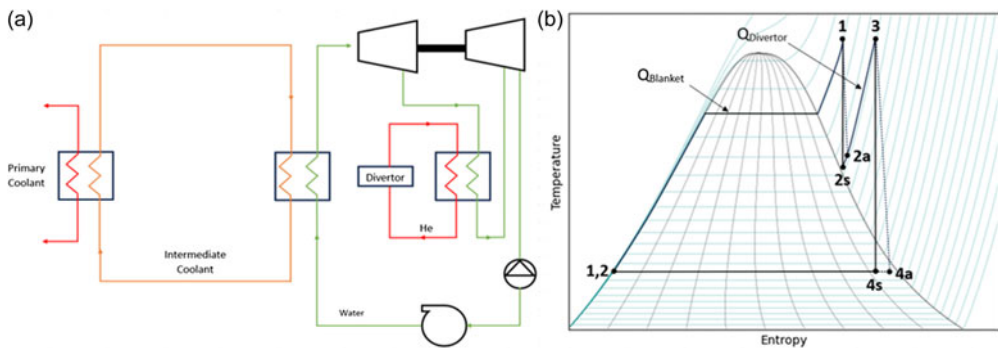


FIGURE 17. (a) The T-S diagram of Rankine cycle. (b) Scheme of Rankine cycle with reheat.

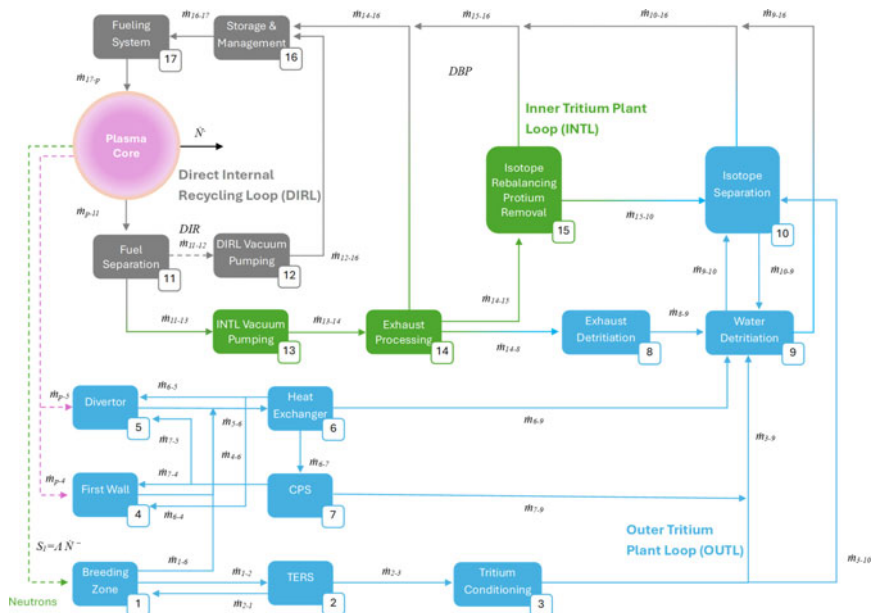


FIGURE 18. Three-loop architecture based the EU DEMO preconceptual design.

REFERENCES

- ABDOU, M., MORLEY, N.B., SMOLENTSEV, S., YING, A., MALANG, S., ROWCLIFFE, A. & ULRICKSON, M. 2015 Blanket/first wall challenges and required R&D on the pathway to DEMO. *Fusion Engng Des.* **100**, 2–43.
- ABDOU, M., RIVA, M., YING, A., DAY, C., LOARTE, A., BAYLOR, L.R., HUMRICKHOUSE, P., FUERST, T.F. & CHO, S. 2021 Physics and technology considerations for the deuterium–tritium fuel cycle and conditions for tritium fuel self sufficiency. *Nucl. Fusion* **61** (1), 013001.
- ABDOU, M., SZE, D., WONG, C., SAWAN, M., YING, A., MORLEY, N.B. & MALANG, S. 2005 US Plans and strategy for ITER blanket testing. *Fusion Sci. Technol.* **47** (3), 475–487.
- AIELLO, G., AUBERT, J., JONQUÈRES, N., LI PUMA, A., MORIN, A. & RAMPAL, G. 2014 Development of the helium cooled lithium lead blanket for DEMO. *Fusion Engng Des.* **89** (7–8), 1444–1450.
- AUBERT, J. *et al.* 2018, Status of the EU DEMO HCLL breeding blanket design development. *Fusion Engng Des.* **136**, 1428–1432.
- BAALRUD, S., FERRARO, N., GARRISON, L., HOWARD, N., KURANZ, C., SARFF, J. & SOLOMON, W. 2020 A community plan for fusion energy and discovery plasma sciences. arXiv 2020, 1–186.
- BADALASSI, V. 2024 Digital twins in fusion & the FERMI project. Oak Ridge National Lab (ORNL).
- BAE, J.W., PETERSON, E. & SHIMWELL, J. 2022 ARC reactor neutronics multi-code validation. *Nucl. Fusion* **62** (6), 066016.
- BARUCCA, L. *et al.* 2021 Pre-conceptual design of EU DEMO balance of plant systems: objectives and challenges. *Fusion Engng Des.* **169**, 112504.
- BHARDWAJ, D., CHENG, B., SPROUSTER, D.J., CUNNINGHAM, W.S., RANI, N., TRELEWICZ, J.R. & SNEAD, L.L. 2024 Fabrication of neutron absorbing metal hydride entrained ceramic matrix shield composites. *Frontiers Nucl. Engng* **3**, 1–12.
- BHATTACHARYA, A., ZINKLE, S.J., HENRY, J., LEVINE, S.M., EDMONDSON, P.D., GILBERT, M.R., TANIGAWA, H. & KESSEL, C.E. 2022 Irradiation damage concurrent challenges with RAFM and ODS steels for fusion reactor first-wall/blanket: a review. *J. Phys.: Energy* **4** (3), 034003.
- BOULLON, R., AUBERT, J., AIELLO, G., JABOULAY, J.-C. & MORIN, A. 2019 The DEMO helium cooled lithium lead “advanced-plus” breeding blanket: design improvement and FEM studies. *Fusion Engng Des.* **146**, 2026–2030.
- BOULLON, R., JABOULAY, J.-C. & AUBERT, J. 2021 Molten salt breeding blanket: investigations and proposals of pre-conceptual design options for testing in DEMO. *Fusion Engng Des.* **171**, 112707.
- CHRISTENSON, M., MOYNIHAN, C. & RUZIC, D.N. 2018 A distillation column for hydrogen isotope removal from liquid lithium. *Fusion Engng Des.* **135**, 81–87.
- Commonwealth Fusion Systems. 2024 ARPA-E award boosts CFS’ quest for the best fusion power plant materials [Internet]. Massachusetts USA: Commonwealth Fusion Systems; [updated 2024, cited 2024 Dec 8]. Available from: <https://cfs.energy/news-and-media/arpa-e-award-boosts-cfs-quest-for-the-best-fusion-power-plant-materials>.
- CRISTESCU, I. & DRAGHIA, M. 2020 Developments on the tritium extraction and recovery system for HCPB. *Fusion Engng Des.* **158**, 111558.
- DAVIES, A.W. & MURPHY, S.T. 2021 Fundamental properties of octalithium plumbate ceramic breeder material. *J. Nucl. Mater.* **552**, 152982.
- DAVIS, A., HARB, M., EL-GUEBALY, L., WILSON, P. & MARRIOTT, E. 2018 Neutronics aspects of the FESS-FNSF. *Fusion Engng Des.* **135**, 271–278.
- DAY, C. 2022 The pre-concept design of the DEMO tritium, matter injection and vacuum systems. *Fusion Engng Des.* **179**, 113139.
- EL-GUEBALY, L. *et al.* 2008 Designing ARIES-CS compact radial build and nuclear system: neutronics, shielding, and activation. *Fusion Sci. Technol.* **54** (3), 747–770.
- EL-GUEBALY, L., RAFFRAY, R., MALANG, S., LYON, J.F. & KU, L.P. 2005 Benefits of radial build minimization and requirements imposed on ARIES compact stellarator design. *Fusion Sci. Technol.* **47** (3), 432–439.
- EL-GUEBALY, L.A. 2018 Nuclear assessment to support ARIES power plants and next-step facilities: emerging challenges and lessons learned. *Fusion Sci. Technol.* **74** (4), 340–369.

- FEDERICI, G. *et al.* 2014 Overview of EU DEMO design and R&D activities. *Fusion Engng Des.* **89** (7–8), 882–889.
- FERRY, S.E., WOLLER, K.B., PETERSON, E.E., SORENSSEN, C. & WHYTE, D.G. 2023 The LIBRA experiment: investigating robust tritium accountancy in molten FLiBe exposed to a D-T fusion neutron spectrum. *Fusion Sci. Technol.* **79** (1), 13–35.
- GAISIN, R. *et al.* 2020 Synthesis of Be₁₂Ti compound via arc melting or hot isostatic pressing. *J. Alloys Compounds* **818**, 152919.
- GARCINUÑO, B., RAPISARDA, D., ANTUNES, R., UTILI, M., FERNÁNDEZ-BERCERUELO, I., SANZ, J. & IBARRA, A. 2018 The tritium extraction and removal system for the DCLL-DEMO fusion reactor. *Nucl. Fusion* **58** (9), 095002.
- GATES, D.A. *et al.* 2018 Stellarator research opportunities: a report of the national stellarator coordinating committee. *J. Fusion Energy* **37** (1), 51–94.
- GIANCARLI, L., GOLFIER, H., NISHIO, S., RAFFRAY, R., WONG, C. & YAMADA, R. 2002 Progress in blanket designs using SiCf/SiC composites. *Fusion Engng Des.* **61–62**, 307–318.
- GIANCARLI, L.M. *et al.* 2020 Overview of recent ITER TBM Program activities. *Fusion Engng Des.* **158**, 111674.
- GOHAR, Y., MAJUMDAR, S. & SMITH, D. 2000 High power density self-cooled lithium–vanadium blanket. *Fusion Engng Des.* **49–50**, 551–558.
- HAMBY, D.M. 1994 A review of techniques for parameter sensitivity analysis of environmental models. *Environ. Monitoring Assess.* **32** (2), 135–154.
- HÄUSSLER, A., WARMER, F. & FISCHER, U. 2018 Neutronics analyses for a stellarator power reactor based on the HELIAS concept. *Fusion Engng Des.* **136**, 345–349.
- HEGNA, C.C. *et al.* 2025 The Infinity Two Fusion Pilot Plant baseline plasma physics design. *J. Plasma Phys.* **2025**, 1–44.
- HERNÁNDEZ, F., PERESLAVTSEV, P., KANG, Q., NORAJITRA, P., KISS, B., NÁDASI, G. & BITZ, O. 2017 A new HCPB breeding blanket for the EU DEMO: evolution, rationale and preliminary performances. *Fusion Engng Des.* **124**, 882–886.
- HERNÁNDEZ, F.A. *et al.* Guangming 2023 Advancements in designing the DEMO driver blanket system at the EU DEMO pre-conceptual design phase: overview challenges and opportunities. *J. Nucl. Engng* **4** (3), 565–601.
- HERNÁNDEZ, F.A. *et al.* 2019 Advancements in the helium-cooled pebble bed breeding blanket for the EU DEMO: holistic design approach and lessons learned. *Fusion Sci. Technol.* **75** (5), 352–364.
- HERNÁNDEZ, F.A. *et al.* 2020 Consolidated design of the HCPB breeding blanket for the pre-conceptual design phase of the EU DEMO and harmonization with the ITER HCPB TBM program. *Fusion Engng Des.* **157**, 111614.
- HERNÁNDEZ, F.A. & PERESLAVTSEV, P. 2018 First principles review of options for tritium breeder and neutron multiplier materials for breeding blankets in fusion reactors. *Fusion Engng Des.* **137**, 243–256.
- HESCH, K., BOCCACCINI, L.V. & STIEGLITZ, R. 2018 Blankets – key element of a fusion reactor – functions, design and present state of development. *Kerntechnik* **83** (3), 241–250.
- HUMRICKHOUSE, P.W. & MERRILL, B.J. 2018 Tritium aspects of the fusion nuclear science facility. *Fusion Engng Des.* **135**, 302–313.
- JABOULAY, J.-C., AIELLO, G., AUBERT, J. & BOULLON, R. 2019 Nuclear analysis of the HCLL “Advanced-Plus” breeding blanket with single module segment structure. *Fusion Engng Des.* **146**, 162–167.
- JIN, X. & YIN, Y. 2017 RAMI comparison of two China test blanket modules. *Ann. Nucl. Energy* **110**, 438–442.
- JOHNSON, C.E., KUMMERER, K.R. & ROTH, E. 1988 Ceramic breeder materials. *J. Nucl. Mater.* **155–157**, 188–201.
- KESSEL, C.E. *et al.* 2015 The ARIES advanced and conservative tokamak power plant study. *Fusion Sci. Technol.* **67** (1), 1–21.
- KESSEL, C.E. *et al.* 2018 Overview of the fusion nuclear science facility, a credible break-in step on the path to fusion energy. *Fusion Engng Des.* **135**, 236–270.

- KIRILLOV, I.R., DANILOV, I.V., SIDORENKOV, S.I., STREBKOV, YUS., MATTAS, R.F., GOHAR, Y., HUA, T.Q. & SMITH, D.L. 1998 Liquid lithium self-cooled breeding blanket design for ITER. *Fusion Engng Des.* **39–40**, 669–674.
- KOLBASOV, B.N., KHRIPUNOV, V.I. & BIRYUKOV, A.Y. 2016 On use of beryllium in fusion reactors: resources, impurities and necessity of detritiation after irradiation. *Fusion Engng Des.* **109–111**, 480–484.
- KOVARI, M., COLEMAN, M., CRISTESCU, I. & SMITH, R. 2018 Tritium resources available for fusion reactors. *Nucl. Fusion* **58** (2), 026010.
- LEYS, O., LEYS, J.M. & KNITTER, R. 2021 Current status and future perspectives of EU ceramic breeder development. *Fusion Engng Des.* **164**, 112171.
- LI, Y. 2024 *Tokamak Energy Advances Development of Vanadium Alloys for Fusion Breeder Blankets*. Vanitec. <https://vanitec.org/latest-from-vanitec/article/tokamak-energy-advances-development-of-vanadium-alloys-for-fusion-breeder-blankets>
- LONGHURST, G.R. *et al.* 2011 Managing beryllium in nuclear facility applications. *Nucl. Technol.* **176** (3), 430–441.
- LORD, M., BENNETT, I., HARRINGTON, C., COOPER, A., LEE-LANE, D., CURETON, A., OLDE, C., THOMPSON, M., JAYASUNDARA, D. & MEATYARD, T. 2024 Fusing together an outline design for sustained fuelling and tritium self-sufficiency. *Phil. Trans. R. Soc. Lond. A: Math. Phys. Engng Sci.* **382** (2280)
- LYYTINEN, T., SNICKER, A., VIRTANEN, J., PALERMO, I., ALGUACIL, J., BOGAARTS, T. & WARMER, F. 2024 Proof-of-principle of parametric stellarator neutronics modeling using Serpent2. *Nucl. Fusion* **64** (7), 076042.
- MALANG, S. & MATTAS, R. 1995 Comparison of lithium and the eutectic lead-lithium alloy, two candidate liquid metal breeder materials for self-cooled blankets. *Fusion Engng Des.* **27** (1–2), 399–406.
- MARONI, V.A., WOLSON, R.D. & STAAHL, G.E. 1975 Some preliminary considerations of a molten-salt extraction process to remove tritium from liquid lithium fusion reactor blankets. *Nucl. Technol.* **25** (1), 83–91.
- MATTAS, R.F., SMITH, D.L., REED, C.B., PARK, J.H., KIRILLOV, I.R., STREBKOV, YUS., RUSANOV, A.E. & VOTINOV, S.N. 1998 Results of R&D for lithium/vanadium breeding blanket design. *Fusion Engng Des.* **39–40**, 659–668.
- MEIER, W.R. 2014 Assessment of tritium breeding blankets from a systems perspective - status report. Tech. Rep, Lawrence Livermore National Laboratory, Livermore, CA.
- MELICHAR, T., FRÝBORT, O., VÁLA, L., ZÁCHA, P., FERNÁNDEZ, I. & RAPISARDA, D. 2017 Optimization of the first wall helium cooling system of the European DCLL using CFD approach. *Fusion Engng Des.* **124**, 426–431.
- MESCHINI, S., FERRY, S.E., DELAPORTE-MATHURIN, RÉMI & WHYTE, D.G. 2023 Modeling and analysis of the tritium fuel cycle for ARC- and STEP-class D-T fusion power plants. *Nucl. Fusion* **63** (12), 126005.
- MORENO, C., BADER, A. & WILSON, P. 2024 ParaStell: parametric modeling and neutronics support for stellarator fusion power plants. *Frontiers Nucl. Engng* **3**, 1–13.
- MUROGA, T., CHEN, J.M., CHERNOV, V.M., KURTZ, R.J. & LE FLEM, M. 2014 Present status of vanadium alloys for fusion applications. *J. Nucl. Mater.* **455** (1–3), 263–268.
- MUROGA, T., TANAKA, T., KONDO, M., NAGASAKA, T. & XU, Q. 2009 Characterization of liquid lithium blanket with RAFM and V-alloy for TBM and DEMO. *Fusion Sci. Technol.* **56** (2), 897–901.
- NAJMABADI, F. *et al.* 2008 The ARIES-CS compact stellarator fusion power plant. *Fusion Sci. Technol.* **54** (3), 655–672.
- NI, M., WANG, Y., YUAN, B., JIANG, J. & WU, Y. 2013 Tritium supply assessment for ITER and DEMOnstration power plant. *Fusion Engng Des.* **88** (9–10), 2422–2426.
- PALERMO, I. *et al.* 2024 Challenges towards an acceleration in stellarator reactors engineering: the dual coolant lithium–lead breeding blanket helical-axis advanced stellarator case. *Energy* **289**, 129970.
- PALERMO, I., WARMER, F. & HÄUSSLER, A. 2021 Nuclear design and assessments of helical-axis advanced stellarator with dual-coolant lithium-lead breeding blanket: adaptation from DEMO tokamak reactor. *Nucl. Fusion* **61** (7), 076019.

- PEARSON, R., BAUS, C., KONISHI, S., MUKAI, K., D'ANGIO, A. & TAKEDA, S. 2022 Overview of kyoto fusionneering's SCYLLA© ("Self-cooled yuryo lithium-lead advanced") blanket for commercial fusion reactors. *IEEE Trans. Plasma Sci.* **50** (11), 4406–4412.
- PERESLAVTSEV, P., HERNÁNDEZ, F.A., ZHOU, G., LU, L., WEGMANN, C. & FISCHER, U. 2019 Nuclear analyses of solid breeder blanket options for DEMO: status, challenges and outlook. *Fusion Engng Des.* **146**, 563–567.
- PIET, S.J., JEPPSON, D.W., MUHLESTEIN, L.D., KAZIMI, M.S. & CORRADINI, M.L. 1987 Liquid metal chemical reaction safety in fusion facilities. *Fusion Engng Des.* **5** (3), 273–298.
- PINT, B.A., EVANGELIA (LILA) K., DINO S., & PAUL H. 2024 "Materials Assessment for FLiBe Fusion Blankets." Oak Ridge National Laboratory (ORNL), Oak Ridge, TN (United States). ORNL/TM-2024/3508. <https://www.osti.gov/biblio/2455087>. September 1, 2024.
- RAFFRAY, A.R., AKIBA, M., CHUYANOV, V., GIANCARLI, L. & MALANG, S. 2002 Breeding blanket concepts for fusion and materials requirements. *J. Nucl. Mater.* **307-311**, 21–30.
- RAPISARDA, D., FERNÁNDEZ-BERCERUELO, I., GARCÍA, A., GARCÍA, J.M., GARCINUÑO, B., GONZÁLEZ, M., MORENO, C., PALERMO, I., URGORRI, F.R. & IBARRA, A. 2021 The European dual coolant lithium lead breeding blanket for DEMO: status and perspectives. *Nucl. Fusion* **61** (11), 115001.
- REYES, S., ANKLAM, T., MEIER, W., CAMPBELL, P., BABINEAU, D., BECNEL, J., TAYLOR, C. & COONS, J. 2016 Recent developments in IFE safety and tritium research and considerations for future nuclear fusion facilities. *Fusion Engng Des.* **109-111**, 175–181.
- ROMANO, P.K., HORELIK, N.E., HERMAN, B.R., NELSON, A.G., FORGET, B. & SMITH, K. 2015 OpenMC: a state-of-the-art Monte Carlo code for research and development. *Ann. Nucl. Energy* **82**, 90–97.
- ROMEDENNE, M., ZHANG, Y., SU, Y.-F. & PINT, B. 2023 Evaluation of the interaction between SiC, pre-oxidized FeCrAlMo with aluminized and pre-oxidized Fe-8Cr-2W in flowing PbLi. *J. Nucl. Mater.* **581**, 154465.
- SAGARA, A. *et al.* 1997 Blanket design using FLiBe in helical-type fusion reactor FFHR. *J. Nucl. Mater.* **248**, 147–152.
- SAMOLYUK, G.D. & EDMONDSON, P.D. 2021 First principles study of the stability and thermal conductivity of novel li-be hybrid ceramics. *Acta Mater.* **215**, 117052.
- SCAFFIDI-ARGENTINA, F., LONGHURST, G.R., SHESTAKOV, V. & KAWAMURA, H. 2000 The status of beryllium technology for fusion. *J. Nucl. Mater.* **283-287**, 43–51.
- SCHWENZER, J.C., DAY, C., GIEGERICH, T. & SANTUCCI, A. 2022 Operational tritium inventories in the EU-DEMO fuel cycle. *Fusion Sci. Technol.* **78** (8), 664–675.
- SEGANTIN, S., MESCHINI, S., TESTONI, R. & ZUCCHETTI, M. 2022 Preliminary investigation of neutron shielding compounds for ARC-class tokamaks. *Fusion Engng Des.* **185**, 113335.
- SEGANTIN, S., TESTONI, R., HARTWIG, Z., WHYTE, D. & ZUCCHETTI, M. 2020 Optimization of tritium breeding ratio in ARC reactor. *Fusion Engng Des.* **154**, 111531.
- SHARAFAT, S., WILLIAMS, B., GHONIEM, N., GHONIEM, A., SHIMADA, M. & YING, A. 2016 Development of a new cellular solid breeder for enhanced tritium production. *Fusion Engng Des.* **109-111**, 119–127.
- SHIMWELL, J. 2021 OpenMC plasma sources. GitHub. <https://github.com/fusion-energy/openmc-plasma-source>. Accessed August 2024.
- SHIMWELL, J., LILLEY, S., MORGAN, L., PACKER, L., KOVARI, M., ZHENG, S. & MCMILLAN, J. 2016 Reducing beryllium content in mixed bed solid-type breeder blankets. *Fusion Engng Des.* **109-111**, 1564–1568.
- SI, C., LU, W., JI, J., ZHANG, S., YAO, X., WANG, W. & CHU, D. 2020 Review on the compatibility of fusion reactor structural materials with high-temperature liquid metals. *J. Phys.: Conf. Ser.* **1637**, 012037.
- SIMON, P.-C.A., HUMRICKHOUSE, P.W. & LINDSAY, A.D. 2022 Tritium transport modeling at the pore scale in ceramic breeder materials using TMAP8. *IEEE Trans. Plasma Sci.* **50** (11), 4465–4471.
- SMITH, D.L., BAKER, C.C., SZE, D.K., MORGAN, G.D., ABDOL, M.A., PIET, S.J., SCHULTZ, K.R., MOIR, R.W. & GORDON, J.D. 1985 Overview of the blanket comparison and selection study. *Fusion Technol.* **8** (1P1), 10–44.

- SMITH, D.L., NATESAN, K., PARK, J.-H., REED, C.B. & MATTAS, R.F. 2000 Development of electrically insulating coatings on vanadium alloys for lithium-cooled blankets. *Fusion Engng Des.* **51–52**, 185–192.
- SMOLENTSEV, S. 2021 Physical background, computations and practical issues of the magnetohydrodynamic pressure drop in a fusion liquid metal blanket. *Fluids* **6** (3), 110.
- SMOLENTSEV, S., MORLEY, N.B., ABDOL, M.A. & MALANG, S. 2015 Dual-coolant lead–lithium (DCLL) blanket status and R&D needs. *Fusion Engng Des.* **100**, 44–54.
- SMOLENTSEV, S., RHODES, T., PULUGUNDA, G., COURTESSOLE, C., ABDOL, M., MALANG, S., TILLACK, M. & KESSEL, C. 2018 MHD thermohydraulics analysis and supporting R&D for DCLL blanket in the FNSF. *Fusion Engng Des.* **135**, 314–323.
- SORBOM, B.N. *et al.* 2015 ARC: a compact, high-field, fusion nuclear science facility and demonstration power plant with demountable magnets. *Fusion Engng Des.* **100**, 378–405.
- STORK, D. *et al.* 2014 Materials R&D for a timely DEMO: key findings and recommendations of the EU roadmap materials assessment group. *Fusion Engng Des.* **89** (7–8), 1586–1594.
- SYBLIK, J., VESELY, L., ENTLER, S., STEPANEK, J. & DOSTAL, V. 2019 Analysis of supercritical CO₂ Brayton power cycles in nuclear and fusion energy. *Fusion Engng Des.* **146**, 1520–1523.
- SZE, D.-K. *et al.* 1998 The ARIES-RS power core—recent development in Li/V designs. *Fusion Engng Des.* **41** (1–4), 371–376.
- SZE, D.K., JUNG, J., CHENG, E.T., PIET, S. & KLEIN, A. 1986 Conceptual design of a self-cooled FLiBe blanket. *Fusion Technol.* **10** (3P2A), 624–632.
- TEPROVICH, J.A., MERCADO, C., HECTOR, R., OLSON, L., GANESAN, P., BABINEAU, D. & GARCIA-DIAZ, B.L. 2019 Electrochemical extraction of hydrogen isotopes from Li/LiT mixtures. *Fusion Engng Des.* **139**, 1–6.
- TILLACK, M.S., BRINGUIER, S.A., HOLMES, I., HOLLAND, L., SANTOS-NOVAIS, F. & MALDONADO, G.I. 2022 GAMBL – a dual-cooled fusion blanket using SiC-based structures. *Fusion Engng Des.* **180**, 113155.
- TILLACK, M.S., HUMRICKHOUSE, P.W., MALANG, S. & ROWCLIFFE, A.F. 2015 The use of water in a fusion power core. *Fusion Engng Des.* **91**, 52–59.
- TILLACK, M.S., MALANG, S., WAGANER, L., WANG, X.R., SZE, D.K., EL-GUEBALY, L., WONG, C.P.C., CROWELL, J.A., MAU, T.K. & BROMBERG, L. 1997 Configuration and engineering design of the ARIES-RS tokamak power plant. *Fusion Engng Des.* **38** (1–2), 87–113.
- U.S. Fusion Materials Coordinating Committee. 2024 Draft of the U.S. Fusion Materials Community Roadmap. September 2024.
- University of Wisconsin-Madison. 2024a Advanced Research Innovation and Evaluation Study (ARIES) program. <https://fti.neep.wisc.edu/fti.neep.wisc.edu/research/aries.html>. Updated 2014. Accessed 2024.
- University of Wisconsin-Madison. 2024b The Center for High Throughput Computing (CHTC). <https://chtc.cs.wisc.edu/>. Accessed 2024.
- UNTERRAINER, R., FISCHER, D.X., LORENZ, A. & EISTERER, M. 2022 Recovering the performance of irradiated high-temperature superconductors for use in fusion magnets. *Superconductor Sci. Technol.* **35** (4), 04LT01.
- US Department of Energy, Fusion Energy Sciences Advisory Committee. 2021 Powering the Future Fusion & Plasmas: A long-range plan to deliver fusion energy and to advance plasma science. Available from: <https://www.osti.gov/biblio/1995209>
- VAN DER LAAN, J.G., KAWAMURA, H., ROUX, N. & YAMAKI, D. 2000 Ceramic breeder research and development: progress and focus. *J. Nucl. Mater.* **283–287**, 99–109.
- VAN DER LAAN, J.G., REIMANN, J. & FEDOROV, A.V. 2016 Ceramic breeder materials. In *Comprehensive Nuclear Materials* **4**, 114–175. Elsevier
- WANG, S., HERNÁNDEZ, F.A., CHEN, H. & ZHOU, G. 2019 Thermal-hydraulic analysis of the First Wall of a CO₂ cooled pebble bed breeding blanket for the EU-DEMO. *Fusion Engng Des.* **138**, 379–394.
- WANG, X.R., TILLACK, M.S., KOEHLI, C., MALANG, S., TOUDESCHI, H.H., NAJMABADI, F. & ARIES Team 2015 ARIES-ACT2 DCLL power core design and engineering. *Fusion Sci. Technol.* **67** (1), 193–219.

- WARMER, F., BEIDLER, C.D., DINKLAGE, A. & WOLF, R. 2016 From W7-X to a HELIAS fusion power plant: motivation and options for an intermediate-step burning-plasma stellarator. *Plasma Phys. Control. Fusion* **58** (7), 074006.
- WHYTE, D.G., DELAPORTE-MATHURIN, R., FERRY, S.E. & MESCHINI, S. 2023 Tritium burn efficiency in deuterium–tritium magnetic fusion. *Nucl. Fusion* **63** (12), 126019.
- WONG, C.P.C. *et al.* 2005 Assessment of first wall and blanket options with the use of liquid breeder. *Fusion Sci. Technol.* **47** (3), 502–509.
- WU, P., MA, Y., GAO, C., LIU, W., SHAN, J., HUANG, Y., WANG, J., ZHANG, D. & RAN, X. 2020 A review of research and development of supercritical carbon dioxide Brayton cycle technology in nuclear engineering applications. *Nucl. Engng Des.* **368**, 110767.
- ZHENG, S. & WU, Y. 2003 Neutronic comparison of tritium-breeding performance of candidate tritium-breeding materials. *Plasma Sci. Technol.* **5** (5), 1995–2000.
- ZHOU, G., HERNÁNDEZ, F.A., KANG, Q. & PERESLAVTSEV, P. 2019 Progress on the helium cooled molten lead ceramic breeder concept, as a near-term alternative blanket for EU DEMO. *Fusion Engng Des.* **146**, 1029–1034.
- ZHOU, G., HERNÁNDEZ, F.A., PERESLAVTSEV, P., KISS, B., RETHEESH, A., MAQUEDA, L. & PARK, J.H. 2023a The European DEMO helium cooled pebble bed breeding blanket: design status at the conclusion of the pre-concept design phase. *Energies* **16** (14), 5377.
- ZHOU, G., REY, J., HERNÁNDEZ, F.A., ABOU-SENA, A., LUX, M., ARBEITER, F., SCHLINDWEIN, G. & SCHWAB, F., 2023b Engineering design of the european DEMO HCPB breeding blanket breeder zone mockup. *Appl. Sci.* **13** (4), 2081.
- ZINKLE, S.J., BOUTARD, J.L., HOELZER, D.T., KIMURA, A., LINDAU, R., ODETTE, G.R., RIETH, M., TAN, L. & TANIGAWA, H. 2017 Development of next generation tempered and ODS reduced activation ferritic/martensitic steels for fusion energy applications. *Nucl. Fusion* **57** (9), 092005.
- ZINKLE, S.J. & GHONIEM, N.M. 2000 Operating temperature windows for fusion reactor structural materials. *Fusion Engng Des.* **51–52**, 55–71.
- ZINKLE, S.J., MÖSLANG, A., MUROGA, T. & TANIGAWA, H. 2013 Multimodal options for materials research to advance the basis for fusion energy in the ITER era. *Nucl. Fusion* **53** (10), 104024.
- ZINKLE, S.J. & SNEAD, L.L. 2014 Designing radiation resistance in materials for fusion energy. *Ann. Rev. Mater. Res.* **44** (1), 241–267.
- ZINKLE, S.J. & WAS, G.S. 2013 Materials challenges in nuclear energy. *Acta Mater.* **61** (3), 735–758.